Published in final edited form as:
*Neuroscience*. 2009 September 15; 162(4): 1377–1397. doi:10.1016/j.neuroscience.2009.05.063.

# Locomotor Networks are Targets of Modulation by Sensory Transient Receptor Potential Vanilloid 1 and Transient Receptor Potential Melastatin 8 Channels

**S. Mandadi**[a], **S. T. Nakanishi**[a], **Y. Takashima**[b], **A. Dhaka**[c], **A. Patapoutian**[d], **D. D. McKemy**[b], and **P. J. Whelan**[a,*]

[a]Hotchkiss Brain Institute, 3330 Hospital Drive Northwest, Calgary, AB, T2N 4N1 Canada

[b]Department of Biological Sciences, Neurobiology Section, University of Southern California, Los Angeles, CA 90089, USA

[c]Department of Biological Structure, University of Washington, Seattle, WA 98195, USA

[d]Department of Cell Biology, The Scripps Research Institute, La Jolla, CA 92037, USA

## Abstract

It is well recognized that proprioceptive afferent inputs can control the timing and pattern of locomotion. C and A$\delta$ afferents can also affect locomotion but an unresolved issue is the identity of the subsets of these afferents that encode defined modalities. Over the last decade, the transient receptor potential (TRP) ion channels have emerged as a family of non-selective cation conductances that can label specific subsets of afferents. We focus on a class of TRPs known as ThermoTRPs which are well known to be sensor receptors that transduce changes in heat and cold. ThermoTRPs are known to help encode somatosensation and painful stimuli, and receptors have been found on C and A$\delta$ afferents with central projections onto dorsal horn laminae. Here we show, using *in vitro* neonatal mouse spinal cord preparations, that activation of both spinal and peripheral transient receptor potential vanilloid 1 (TRPV1) and transient receptor potential melastatin 8 (TRPM8) afferent terminals modulates central pattern generators (CPGs). Capsaicin or menthol and cooling modulated both sacrocaudal afferent (SCA) evoked and monoaminergic drug-induced rhythmic locomotor-like activity in spinal cords from wild type but not TRPV1-null (*trpv1*$^{-/-}$) or TRPM8-null (*trpm8*$^{-/-}$) mice, respectively. Capsaicin induced an initial increase in excitability of the lumbar motor networks, while menthol or cooling caused a decrease in excitability. Capsaicin and menthol actions on CPGs involved excitatory and inhibitory glutamatergic mechanisms, respectively. These results for the first time show that dedicated pathways of somatosensation and pain identified by TRPV1 or TRPM8 can target spinal locomotor CPGs.

### Keywords

TRP; mouse spinal cord; locomotor rhythm; CPG; capsaicin; menthol

It is now well established that proprioceptive afferent feedback can control the timing and pattern of stepping (Pearson, 2004). This work, which is largely derived from using the cat, has established that both cutaneous (mechanoreceptors) and muscle afferents (load and muscle stretch) project onto reflex pathways that affect pattern generators (Duysens and Pearson, 1976; Lundberg, 1979; Conway et al., 1988; Gossard et al., 1994; Lam and Pearson, 2002).

*Corresponding author. Tel: +1-403-220-4210; fax: +1-403-283-2700. whelan@ucalgary.ca (P. J. Whelan).

On the other hand, data regarding the role of small (C) and medium (A$\delta$) diameter afferents (conduction velocity 2 and ~20 $ms^{-1}$; diameter 0.2–1.0 $\mu$m and 1–5 $\mu$m, respectively) in the control of ongoing locomotion are sparse. Another issue is that C and A$\delta$ afferents are a heterogeneous population subserving several modalities (hot, cold, touch, etc.) (Venkatachalam and Montell, 2007). Part of the issue here, has been the search for the molecular identities of sensors that could classify selective subsets of C and A$\delta$ afferents that modulate central pattern generators (CPGs).

Historically, afferents have been grouped together based on the fact that higher electrical stimulus intensities are required to recruit them. From an early stage, it was recognized and confirmed that high-threshold afferents could access locomotor pattern generating centers within the spinal cord (Jankowska et al., 1967a,b). Eccles and Lundberg initially termed these groups of afferents flexor reflex afferents (FRA) based on their similar polysynaptic effects in motoneurons (Eccles and Lundberg, 1959). Lundberg later suggested that these high-threshold afferents are composed of high-threshold muscle afferents, joint afferents and some cutaneous afferents (Lundberg, 1979). It is also clear that nociceptive afferents can access pattern generators. Evidence collected using decerebrate cats has found that noxious stimulation of the foot can elicit locomotor activity (Schomburg et al., 2001) and FRA stimulation can reset the stepping pattern (Schomburg et al., 1998). Similar observations were made using chronic spinal cats where perineal afferent stimulation was used to train the cats for treadmill locomotion (Barthélemy et al., 2007). Moreover, in the *in vitro* neonatal rat spinal cord preparation, it has been found that noxious heat can trigger cycles of locomotor activity, and these patterns are opioid sensitive (Blivis et al., 2007). Therefore, it appears likely that C and A$\delta$ nociceptive afferents do play a role in the control of locomotion. However, a gap in our knowledge has been the identification of the classes of afferents that participate in these effects, specifically those arising from the skin.

Over the last decade, new molecular tools used to identify and activate subsets of C and A$\delta$ nociceptive afferents have been discovered, specifically the transient receptor potential (TRP) superfamily of non-selective cation channels (Clapham et al., 2005). Within the nervous system, they subserve diverse functions (Nilius, 2007; Nilius et al., 2007); however, we will focus on a class known as ThermoTRPs which are well known to be sensor receptors that transduce changes in heat and cold (Venkatachalam and Montell, 2007). ThermoTRPs are known to help encode somatosensation and painful stimuli, and receptors have been found on both the peripheral and central projections of C and A$\delta$ afferents (Julius and Basbaum, 2001; Levine and Alessandri-Haber, 2007; Willis Jr, 2007). For example, transient receptor potential vanilloid 1 (TRPV1) is an ion channel that is activated by noxious heat (>43 °C) and, more specifically, by capsaicin (Caterina et al., 1997, 2000). On the other hand, transient receptor potential melastatin 8 (TRPM8) is an ion channel present in a predominantly segregated group of primary afferents and is activated by cool temperatures (15–27 °C) as well as menthol (McKemy et al., 2002; Peier et al., 2002; Bautista et al., 2007; Dhaka et al., 2007).

In this paper, we activate TRPV1 and TRPM8 channels and examine their effects on downstream motor networks. We take advantage of our isolated mouse spinal cord preparation where we can elicit locomotor activity by stimulation of sacrocaudal afferents (SCA) (Lev-Tov et al., 2000; Whelan et al., 2000; Bertrand and Cazalets, 2002). Recent work has established that this pathway is opioid sensitive and contains nociceptive afferents (Blivis et al., 2007). To the best of our knowledge, this is the first time that specific nociceptive classes of afferents and their relation to ongoing locomotion have been explored. Some of these data have been presented in abstract form (Mandadi and Whelan, 2007; Mandadi et al., 2008).

## Experimental Procedures

Experiments were performed on Swiss Webster mice (Charles River Laboratories, Senneville, Quebec, Canada), transient receptor potential vanilloid 1-null mice (*trpv1*$^{-/-}$) (B6.129X1-Trpv1tm1Jul/J, The Jackson Laboratory, Bar Harbor, Maine, USA), transient receptor potential melastatin 8-null mice (*trpm8*$^{-/-}$) (generated as described in; Dhaka et al., 2007). Mice used for all experiments in the study were between postnatal days (P) 0 and P3. The animals were anesthetized by hypothermia, decapitated and eviscerated using procedures approved by the University of Calgary Animal Care Committee in conformation with international guidelines on the ethical use of animals. The remaining tissue was placed in a dissection chamber filled with oxygenated (95% $O_2$, 5% $CO_2$) artificial cerebrospinal fluid (ACSF: concentrations in mM: 128 NaCl, 4 KCl, 1.5 $CaCl_2$, 1 $MgSO_4$, 0.5 $Na_2HPO_4$, 21 $NaHCO_3$, 30 D-glucose).

### Isolated spinal cord preparations

A ventral laminectomy exposed the spinal cord sparing as much of the cauda equina as possible, and the ventral and dorsal roots were cut. The cord was transected at thoracic segment 5 (T5) and then was gently removed from the vertebral column. The spinal cord was then transferred to a recording chamber filled with oxygenated ACSF and allowed to equilibrate before being heated to ~27 °C. For SCA-evoked locomotion experiments a split-bath was built with Vaseline walls between spinal cord segments lumbar 6 (L6) and sacral 1 (S1). Drugs were bath applied caudal or rostral to the split bath at L6/S1.

### Slice preparations

The isolated spinal cord was immediately transferred to a pre-cooled (4 °C) slicing chamber and stabilized in an upright position onto an agar block using 20% gelatin. The slicing chamber was then filled with ice cold, oxygenated sucrose–ACSF solution (concentrations in mM: 25 NaCl, 188 sucrose, 1.9 KCl, 10 $MgSO_4$, 1.2 $Na_2HPO_4$, 26 $NaHCO_3$, 25 D-glucose) which was kept chilled and continuously oxygenated. Transverse sections (350 $\mu$m) were cut (Leica Vibrotome VT1000S), and the slices from lumbar segments 4 and 5 were collected in a chamber containing pre-warmed (36 °C) oxygenated recovery ACSF (concentrations in mM: 119 NaCl, 1.9 KCl, 1 $CaCl_2$, 10 $MgSO_4$, 1.2 $Na_2HPO_4$, 26 $NaHCO_3$,10 D-glucose, 1.5 kynurenic acid, 2 lactic acid, 3% dextran). The slices were equilibrated for at least 45 min before being transferred to a holding ACSF (the same solution as recovery ACSF except without kynurenic acid, lactic acid and dextran) and then moved into the recording rig.

### Hind limb–spinal cord preparations

A dorsal and ventral laminectomy exposed the spinal cord sparing as much of the cauda equina as possible. The cord was transected at T5 with the spinal cord attached to a single hind limb by the lumbar and sacral dorsal roots. The remaining thoracic dorsal and ventral roots were cut. The hind limb–spinal cord preparation was then transferred to a recording chamber filled with oxygenated ACSF. A split-bath was built with Vaseline walls to separate the spinal cord portion from the hind paw. The spinal cord portion was equilibrated at room temperature before being heated to ~27 °C. The compartment containing the hind paw was heated to ~32 °C. Control experiments were carried out to eliminate the possibility of effects on the rhythm due to the vehicle (DMSO) or to the injection procedure itself. In order to account for mechanical stimulation of hind paw, the preparation was allowed to equilibrate for 10 min after the needle was introduced. Then, either capsaicin (1 $\mu$M) or vehicle was injected into the dorsal skin of the hind paw. During application of cold stimulus to the hind paw, the preparation was allowed to equilibrate for 10 min at different temperatures and recordings were made for an additional 10 min at each temperature. Cooling (~17 °C) was applied by using pre-cooled ACSF followed by reintroduction of pre-warmed (~32 °C) ACSF. For all experiments with capsaicin or cooling, the spinal cord portion of the bath was always maintained at ~27 °C.

### Electrophysiological recordings and activation of locomotor networks from isolated spinal cord preparations

Neurograms were recorded with suction electrodes into which left and right segmental ventral roots were drawn. Generally, neurograms were recorded from the left and right lumbar 2 (L2) and 5 (L5) ventral roots. The neurograms were amplified (100–20,000 times), filtered (0.1–1 kHz or DC–1 kHz) and digitized (Axon Digidata, 1322A, Molecular Devices, Sunnyvale, CA, USA) for future analysis. Rhythmic alternating segmental L2 neurogram activity along with alternating ipsilateral bursting between the L2 and L5 neurograms was taken to indicate fictive locomotion (Whelan et al., 2000). Constant current stimulus trains (A360 World Precision Instruments, Sarasota, FL, USA; AMPI Master 8 pulse generator, Jerusalem, Israel) were delivered to the sacral 4 (S4) dorsal root through a suction electrode. To determine the stimulus threshold (T), single pulses were delivered at increasing intensities until a polysynaptic reflex response could be just resolved (2–10 $\mu$A). Pulses (250 ms) were delivered every three minutes (4 Hz, 40 pulses, 2 T, 10 s duration) at a constant intensity throughout an experiment (Whelan et al., 2000). Control rhythms were recorded for 15 min before pharmacological agents were added. In certain experiments, pharmacological agents were used to evoke rhythmicity (Jiang et al., 1999; Whelan et al., 2000). These drugs included *N*-methyl-$_{D(L)}$-aspartic acid (NMA, 5 $\mu$M), dopamine (DA, 50 $\mu$M) and 5-HT (10 $\mu$M).

Data were analyzed using custom written programs (MATLAB, MathWorks, Natick, MA, USA) as well as commercially available programs (SigmaStat, Systat, San Jose, CA; Oriana, Kovach Computing Services, Anglesey, UK). We digitally filtered all data (high-pass filter: 100 Hz) for further analysis using MATLAB. For stimulus-evoked activity, we used a spike detection algorithm to digitally blank the stimulus artifacts. Time series analyses of raw data were performed by (i) taking binned intervals of 10 s [electrical stimulation protocol; total data 50 s; five bins] and 60 s [rhythmogenic drugs protocol; 15 bins; total data 15 min], (ii) applying a low-pass digital filter (Chebyshev type I, 100 Hz) and (iii) resampling at 250 Hz. Means were subtracted from the processed data and further smoothed using a digital smoothing polynomial filter (Savitzky-Golay 3rd order, length of segment 250 ms). To analyze the stability and phase of the rhythms, we used time analyses techniques as previously described (Pearson et al., 2003). These techniques are illustrated in Fig. 1. Cross- and autocorrelograms were calculated and the quality of the rhythm along with the cycle period was assessed by measuring the correlation coefficients for pairs of neurograms (left and right L2 or L5). Such analyses were used throughout the study.

Circular statistics and plots were used to describe and assess changes in phase. To analyze and to illustrate phase relationships, we used circular plots in which the phase was normalized from 0 to 1 (Kjaerulff and Kiehn, 1996; Zar, 1999). If the length of the arrow is large, then this suggests a tendency for the rhythms represented by the two neurograms to be coupled. Significance was computed using a modified Rayleigh's test ($P<0.05$), with an expected phase of 0.5. We have presented data from different experiments by using circular plots that summarize the mean phase and *r*-value for each experiment. We then used these values to calculate a group mean phase. In certain cases we tested for differences in phases across conditions. In these cases we made use of a Watson–Williams test, which is a circular statistic equivalent to a *t*-test or ANOVA (Watson and Williams, 1956). Examples of the circular plots and circular statistics used to analyze phase changes in SCA and drug evoked rhythm are shown in Supplementary Figs. 1 and 2, respectively.

To examine changes in amplitude of the neurograms, we averaged smoothed neurograms that were aligned to bursts of a given channel (left L2). Here we used a burst detection algorithm to average bursts across 5-min segments of data before and after addition of agonists. The peak values were then normalized to control burst amplitudes before the bath-application of drugs. Differences were compared using paired Student's *t*-tests or a repeated measures one-way or

two-way ANOVA. In the case of ANOVAs, a post hoc pairwise Tukey's test was performed if significant differences were found ($P<0.05$).

## Immunocytochemistry

TRPM8-GFP transgenic mice were generated and immunocytochemistry was performed as described (Takashima et al., 2007). Briefly, appropriately staged neonatal mice were anesthetized and perfused transcardially with 0.1 M PBS followed by fixative (4% formaldehyde, 0.1 M PBS [pH 7.3] at 4 °C). Spinal cords were carefully dissected out of the animals and post-fixed for 1 h at 4 °C in the same fixative. Samples were washed with 0.1 M PBS for 30 min. All tissues were cryoprotected in 30% sucrose, 0.1 M PBS at 4 °C overnight, quick frozen in OCT, sectioned with a cryostat at 30 $\mu$m, and mounted on Superfrost Plus slides. Slides were stored at −80 °C. Frozen slides were dried at 4 °C for 30 min then at room temperature for 30 min and washed with DI water for 30 s. Slide-mounted sections were washed three times with PBS, once with PBS plus 0.1% Triton X-100 (PBS+TX) for 30 min, and three times with PBS before a blocking step (1 h in PBS+TX containing 20% goat serum). Primary antibodies were diluted in PBS and incubated at 4 °C overnight. These antibodies and dilutions were used: 1:500 rabbit anti-TRPV1 (RA-14113; Neuromics, Edina, MN, USA), 1:1000 chicken anti-GFP (GFP-1020; Aves Laboratories, Tigard, OR, USA), and 1:500 rabbit anti–homeobox gene 9 (Hb9) (Abcam, Cambridge, MA, USA). Sections were washed three times with PBS+TX and incubated for 2 h at room temperature with secondary antibodies conjugated to Alexa-488 or Alexa-568 (Molecular Probes) diluted 1:1000 in blocking solution. Sections were washed five times with PBS+TX and mounted in Vectashield mounting medium with DAPI, or PermaFluor mounting medium (Thermo Scientific, Phoenix, AZ, USA). Digital images were acquired on an Olympus IX70. All antibodies used here have been appropriately characterized for their specificity to detect protein of interest as described and reported in our previous studies (Han et al., 2007; Takashima et al., 2007). Briefly, specificity for the TRPV1 antibody was performed in human embryonic kidney (HEK) cells heterologously expressing either mouse *trpv1* or empty vector (pcDNA3). Under these conditions, there was no signal with the TRPV1 antibody in cells expressing empty vector pcDNA3. For TRPM8 labeling, the GFP antibodies used were specific to stain only axonal tracer eGFP driven by the TRPM8 transcriptional promoter. For the TRPV1 and Hb9 immunohistochemistry experiments, we excluded the primary antibodies to serve as negative controls.

## Whole cell recordings

The spinal cord slice from lumbar segments 4 or 5 was placed into the recording chamber and superfused with oxygenated ACSF solution (concentrations in mM: 128 NaCl, 4 KCl, 1.5 $CaCl_2$, 1 $MgSO_4$, 0.5 $Na_2HPO_4$, 21 $NaHCO_3$, 30 D-glucose) at an approximate rate of 2 ml/min. Electrodes were pulled from borosilicate glass on a P87 Flaming/Brown puller (Sutter Instrument, Novato, CA, USA) and had resistances in the range of 3–5 MΩ. The internal pipette solution contained (in mM): 130 K-gluconate, 7 NaCl, 0.1 EGTA, 10 Hepes, 0.3 $MgCl_2$, 2 ATP and 0.5 GTP (adjusted to pH 7.3 with KOH). The liquid junction potential between internal and external solutions was calculated using Clampex software to be 11.7 mV in K-gluconate internal solution and corrected. Motoneurons were visually identified as large diameter soma (>20 $\mu$M) in the ventral horn of the spinal cord for whole-cell patch using differential interference contrast optics and infrared light transmission (BX51, Olympus, Canada Inc., Markham, Ontario, Canada). The data were low pass filtered (10 kHz) and digitized (sampling rate: 20 kHz) for off-line analyses (Digidata, 1322A, Clampex 8 and 10, Molecular Devices). Capsaicin and menthol were bath applied to the slices in the recording chamber. In some experiments immediate effects of capsaicin application on motoneurons were tested in the presence of blockers of fast synaptic transmission (NMDA receptor antagonist APV (100 $\mu$M), AMPA/kainate receptor antagonist CNQX (20 $\mu$M), glycine receptor antagonist strychnine (2 $\mu$M), $GABA_A$ antagonist picrotoxin (50 $\mu$M) and $GABA_B$

antagonist CGP (50 $\mu$M). Current clamp analyses were carried out using Clampfit and step current protocols were analyzed using custom designed MatLab programs. A current injection protocol was used to determine the rheobase of each motoneuron that was defined as the minimum amplitude current step (50 ms) sufficient to elicit the first action potential. The data are presented as mean±SEM with *n*=the number of cells unless indicated otherwise. Wherever necessary, a percentage change was given by normalizing corresponding control value to 100% in each individual cell. Differences were compared using paired Student's *t*-tests or a repeated measures one-way ANOVA. A post hoc pairwise Tukey's test was performed if significant differences were found ($P<0.05$).

### Pharmacology

All the drugs used in this study were purchased from Sigma-Aldrich, St. Louis, MO, USA. Capsaicin (1 $\mu$M) was used to activate TRPV1 and (−)-menthol (100 and 200 $\mu$M) was used to activate TRPM8. The agonist concentrations were established using previous reports and by testing in preliminary experiments whether the effects were reversible following a washout. The drugs used to induce fictive locomotion included: NMA (5 $\mu$M), 5-HT (10 $\mu$M), and DA (50 $\mu$M). The glycine receptor antagonist strychnine (2 $\mu$M), the $GABA_A$ antagonist picrotoxin (50 $\mu$M) and the $GABA_B$ antagonist CGP (50 $\mu$M) were used to block fast inhibitory synaptic transmission and induce a stable synchronous rhythm. The *N*-methyl-D-aspartic acid receptor (NMDAR) antagonist APV (50–100 $\mu$M) and the AMPA receptor (AMPAR) antagonist CNQX (10–40 $\mu$M) were used to inhibit capsaicin-mediated excitatory synaptic transmission onto CPG networks. The metabotropic glutamate receptor (mGluR) type II antagonist, LY341495 (50 $\mu$M), and the mGluR type III antagonist, UBP1112 (50 $\mu$M), were used to block menthol-mediated inhibitory synaptic transmission onto CPG networks. Vehicles for drug stock solutions were capsaicin (DMSO), menthol (ethanol), LY341495 and UBP1112 in 1 M NaOH, and distilled water for all other drugs stock solutions. We tested the vehicle concentrations used (DMSO at 0.001%; ethanol at 0.1%, 1 M NaOH at 0.05%) to rule out any effects of vehicle (data not shown).

## Results

### TRPV1 modulates SCA evoked locomotor rhythm

To address whether modulation of subclasses of C and A$\delta$ afferent inputs alters the excitability of spinal motor circuits, we used a stimulus paradigm which activated SCA (Lev-Tov et al., 2000; Whelan et al., 2000). These afferents likely synapse onto interneurons which project directly or indirectly into the ventrolateral funiculus (VLF) and in turn onto the lumbar CPG (Fig. 2C) (Strauss and Lev-Tov, 2003). We activated the subclass of TRPV1-positive C and A$\delta$ afferents in the SCA pathway by using the TRPV1 agonist capsaicin. To investigate TRPV1-mediated modulation of the SCA evoked locomotor rhythm in an isolated *in vitro* spinal cord preparation, we separately superfused the spinal segments T5–L6 and S1–cauda equina using a split-bath approach (Strauss and Lev-Tov, 2003). A locomotor rhythm was evoked by trains of electrical stimuli (2 T, 4 Hz for 10 s) to the S4 dorsal root and recorded from the L2 and L5 ventral roots (Fig. 2Ai, C). Capsaicin (1 $\mu$M) was bath-applied caudal to the L6/S1 Vaseline split (S1–cauda equina) to investigate if TRPV1 positive C and A$\delta$ afferents contributed to the SCA pathway projecting onto lumbar locomotor CPG networks through the VLF. After five minutes, the evoked rhythm destabilized and became tonic interspersed with irregular bursts (Fig. 2Aii, *n*=5). Ten minutes later, we were no longer able to elicit any rhythmic activity (Fig. 2Aiii, *n*=5). This absence of activity following capsaicin application is likely due to the well-known phenomenon of capsaicin-induced desensitization of TRPV1 (Szolcsányi, 2004; Tominaga and Tominaga, 2005). This suggests that capsaicin-sensitive C and A$\delta$ afferent projections at sacral segments are involved in the modulation of lumbar CPG activity activated by SCA stimulation. Next, we tested whether bath application of capsaicin

to the rostral compartment could produce tonic activity and disrupt the rhythm, and we found that this was true (data not shown, *n*=3). Surprisingly, capsaicin application to the rostral compartment also induced desensitization of the SCA-evoked rhythm. Two possible explanations are 1, capsaicin-sensitive collateral S4 afferent project onto the dorsal horn of segments rostral to the L6/S1 split or 2, there is TRPV1 expression in VLF interneurons. We confirmed that the TRPV1 expression was limited to the dorsal horn of sacral and lumbar segments, with no expression in the ventral horn or white matter regions of the spinal cord (Fig. 4). This result does not support the possibility of a direct modulation of ventral horn motor networks or VLF interneurons by capsaicin. The most parsimonious hypothesis is that TRPV1 S4 afferents project rostral to and beyond L6.

To further test whether capsaicin-induced modulation of the SCA evoked locomotor rhythm was mediated by TRPV1 expressing C and A$\delta$ afferents, we used *in vitro* spinal cord preparations from *trpv1*$^{-/-}$. Capsaicin (1 $\mu$M) applied to either the caudal (Fig. 2Bi-iii, *n*=5) or rostral (data not shown, *n*=3) compartments did not have any effect on any of the parameters used to examine rhythmic output (Phase: Watson–Williams, *P*>0.5; peak-to-trough correlation coefficient [PTCC]: L2–L5, *P*>0.5; AC max: L2 and L5, *P*>0.5; Cycle Period, *P*>0.5).

## Menthol modulates SCA evoked locomotor rhythm via TRPM8

To identify other subclasses of C and A$\delta$ afferents as components of the SCA locomotor pathway, we targeted menthol-sensitive neurons that express TRPM8, using the isolated *in vitro* spinal cord preparation. A locomotor rhythm was elicited by trains of electrical stimuli (2 T, 4 Hz for 10 s) delivered to the S4 dorsal root and the activity was recorded from the L2 and L5 ventral roots (Fig. 3Ai, Bi and E). Menthol (100 and 200 $\mu$M) was bath-applied to the caudal (S1–cauda-equina) or rostral (T5–L6) compartments. After 15 min of menthol application to the caudal compartment, no effect was seen on the cycle period or amplitude of the evoked rhythm (Fig. 3Aii–iii, *n*=3). There was no significant change in the phase of rhythm between segmental L2 and ipsilateral L2–L5 neurograms (Watson–Williams, *P*>0.5; Fig. 3D). Higher concentrations of menthol (500 $\mu$M) were not used due to nonspecific direct effects on motoneurons (data not shown, *n* = 3). Nonetheless, these data suggest an absence of menthol-sensitive modulation of C and A$\delta$ afferents projecting onto sacral segments in the SCA pathway (Fig. 3E). In contrast, rostral application of menthol at 200 $\mu$M but not 100 $\mu$M produced a slowing of the rhythm characterized by a significant increase in the cycle period and a significant decrease in amplitude (Fig. 3Bii, Biii, 3D). No significant changes in the phase lag between neurograms following menthol application to the rostral compartment were observed (Watson–Williams, *P*>0.1). PTCC (L2–L5, *P*>0.5) or AC max (L2, *P*>0.5; L5, *P*>0.1) values between control and menthol treatments were not significant.

Next, to show that rostral menthol-induced modulation of the SCA-evoked locomotor rhythm was mediated by TRPM8 expressing C and A$\delta$ afferents, we used *in vitro* spinal cord preparations from *trpm8*$^{-/-}$ mice. Menthol (100 and 200 $\mu$M) bath-applied to the rostral compartment (T5– L6) had no effect on the cycle period of the SCA-evoked rhythm (*P*>0.5, Fig. 3C, 3D, *n*=4). Again the quality of the rhythm was not altered by menthol (PTCC, *P*>0.5; AC max: L2, *P*>0.1, L5, *P*>0.1), and no significant changes in the phase lag between neurograms were observed (Watson–Williams, *P*>0.5). These data demonstrate, for the first time, that menthol-induced modulation of the SCA-evoked rhythm is mediated by activation of TRPM8.

## TRPV1 and TRPM8 expression in lumbar and sacral segments

We investigated probable loci of capsaicin or menthol actions based on the expression pattern of TRPV1 and TRPM8 in our spinal cord preparations. In adult rodents, the central projections of TRPV1 and TRPM8 afferents terminate predominantly in the most superficial laminae of

the dorsal horn (Tominaga et al., 1998; Takashima et al., 2007; Dhaka et al., 2008). To confirm a similar distribution in neonatal mice (P0–P3), we performed immunohistochemistry to visualize the central projections of TRPV1-labeled afferents in both the sacral and lumbar spinal cord (Fig. 4, left panel). Robust immunoreactivity for TRPV1 was found in lamina I and II in the dorsal horn of both the lumbar and sacral spinal cord. This labeling was not observed in control experiments in which the primary antibody was excluded (data not shown). Previously, it has been reported that some TRPV1-positive fibers are found deeper in the spinal cord (lamina V and X) in adult rats (Tominaga et al., 1998), but corresponding fibers were not observed in our neonatal preparations. It is unclear if this is due to the differences in developmental age, or if these more ventral projections are beyond the level of detection. Nonetheless, these results agree with previous expression analyses of TRPV1-positive central projections (Tominaga et al., 1998) and demonstrate that the preponderance of these fibers terminate in lamina I and II of the dorsal horn.

To examine the localization of TRPM8-expressing central afferent projections, we took advantage of the TRPM8-GFP transgenic mouse line in which the expression of the axonal tracer eGFP is driven by the TRPM8 transcriptional promoter (Takashima et al., 2007). GFP has been shown to be a reliable reporter of TRPM8 expression in this context. Previous studies have determined that, in adult animals, TRPM8-positive central projections terminate in lamina I and II, as well as in the dorsal midline (Takashima et al., 2007; Dhaka et al., 2008). In P0–P3 transgenic mice, GFP expressing afferents projecting into the dorsal horn of the sacral segments were similarly restricted to the outermost lamina (Fig. 4, middle panel). In contrast to adults, GFP expression was present in the ventral horn midline below the central canal in both lumbar and sacral segments. These data suggest that TRPM8 expression in the spinal cord is developmentally regulated. In contrast to TRPV1, we did observe TRPM8 expression in the ventral horn of lumbar and sacral segments. A small level of co-localization of TRPV1 and TRPM8-GFP (yellow) in the dorsal horn lamina I of both lumbar and sacral segments was observed (Fig. 4, right panel). This confirms previous findings of colocalization of TRPV1 and TRPM8 in adult DRG neurons (Takashima et al., 2007; Dhaka et al., 2008). Also, a fraction of embryonic and neonatal DRG soma expresses both TRPV1 and TRPM8 (Y. Takashima and D. D. McKemy, unpublished observations).

We addressed whether menthol exerts a direct effect on motoneurons and/or candidate CPG interneurons. We examined co-expression of GFP with a transcription factor, Hb9, which is present in motoneurons and ventral horn interneurons (Arber et al., 1999; Thaler et al., 1999). Some Hb9 positive interneurons in lamina VIII have electrophysiological properties consistent with them being members of CPG networks (Arber et al., 1999; Thaler et al., 1999; Hinckley et al., 2005; Wilson et al., 2005). Thus, if TRPM8 is expressed in these cells within the spinal cord, then the effect of menthol on rhythmic activity could be due to direct activation of these cells. We saw that Hb9 immunoreactivity was restricted to a subset of neurons within the ventral horn and along the ventral midline below the central canal (Fig. 5A, 5B), which is consistent with previous studies (Arber et al., 1999; Thaler et al., 1999), in control experiments where the anti-Hb9 primary antibody was omitted, no labeling was observed (data not shown). In double labeling experiments, TRPM8 did not co-localize with Hb9 positive motoneurons (Fig. 5A). We did observe GFP expression in close proximity to Hb9-immunoreactivity cells (Fig. 5B), however there was no evidence of GFP labeled axons projecting to Hb9-immunoreactive neurons.

Thus far, the results suggest that capsaicin or menthol effects on lumbar locomotor activity were mediated by TRPV1 or TRPM8 respectively, and that in the case of TRPV1, the modulation is predominantly occurring at the central terminals of afferent fibers. This prompted us to investigate if the subsets of C and A$\delta$ afferents expressing TRPV1 or TRPM8 could modulate fictive locomotion induced by bath application of rhythmogenic drugs (NMA, 5-HT

and DA) which are well known to induce a stable locomotor rhythm (Whelan et al., 2000). This model allowed us to monitor sensorimotor modulation of CPG function by chemical activation of C and A$\delta$ afferent terminals in the absence of electrical stimulation of primary afferents.

## Capsaicin modulates drug-induced locomotor rhythm via TRPV1

TRPV1-mediated modulation of locomotor CPGs was examined by first inducing a locomotor rhythm by bath applying a combination of rhythmogenic drugs (5 $\mu$M NMA, 10 $\mu$M 5-HT and 50 $\mu$M DA) to the spinal cord (T5-cauda equina) (Fig. 6Ai). After a stable rhythm was established, capsaicin (1 $\mu$M) was bath-applied. Within five minutes, the frequency of the locomotor rhythm increased, as indicated by a decrease in the cycle period ($P<0.05$, Fig. 6Aii, 6 C, $n=5$). Such modulation ceased after 10 min of capsaicin application (Fig. 6Aiii, 6 C, $n=5$). There was no significant change in the amplitude ($P>0.5$, Fig. 6D) or phase (Watson–Williams, $P>0.1$). Capsaicin did not alter the stability of the rhythm (AC max: L2 and L5, $P>0.1$; PTCC, $P>0.5$).

Using *trpv1*$^{-/-}$ mice, we tested whether capsaicin-induced modulation of the drug-induced locomotor rhythm was mediated via TRPV1 expressing C and A$\delta$ afferents. Bath application of capsaicin had no effect on the cycle period or amplitude of the drug-induced locomotor rhythm ($P>0.5$, Fig. 6B, 6C, 6D, $n=3$). There was no significant change in phase across conditions (Watson–Williams, $P>0.5$). Capsaicin did not alter the stability of the rhythm (AC max: L2 and L5, $P>0.5$, PTCC, $P>0.5$). These data confirmed that capsaicin-induced modulation of the drug induced locomotor rhythm was mediated via activation followed by desensitization of TRPV1 expressing C and A$\delta$ afferents sensitive to capsaicin (Fig. 6E) (Tominaga and Tominaga, 2005).

## Menthol modulates drug-induced locomotor rhythm via TRPM8

In the SCA-evoked locomotor rhythm model, TRPM8-mediated modulation of CPG activity was observed only when menthol was applied to the rostral compartment. These data suggest that there could be modulation from the TRPM8 expressing C and A$\delta$ afferent projections onto thoracolumbar segments containing the locomotor CPG. To provide further evidence for this hypothesis, we tested the effects of bath-applied menthol on drug-induced locomotor activity (5 $\mu$M NMA, 10 $\mu$M 5-HT and 50 $\mu$M DA) (Fig. 7Ai). After obtaining a stable rhythm, menthol (100 and 200 $\mu$M) was bath-applied to the whole cord (T5–cauda equina) resulting in a dose-dependent slowing of the alternating rhythmic pattern characterized by a significant increase in cycle period ($P<0.005$, Fig. 7Aii–iii, 7 C, $n=5$). We also observed a significant decrease in the amplitude of the neurogram bursts upon addition of 200 $\mu$M menthol ($P<0.005$, Fig. 7Aiii, 7 D). However, there was no significant change in the stability (PTCC: L2–L5, $P>0.5$; AC max: L2, $P>0.1$, L5, $P>0.1$) or phase of the rhythm (modified Rayleigh's, $P<0.05$; Watson–Williams, $P>0.5$).

To demonstrate that menthol-induced modulation of the drug-induced locomotor rhythm was mediated by TRPM8 expressing C and A$\delta$ afferents, we used *in vitro* spinal cord preparations from *trpm8*$^{-/-}$ mice. In contrast to wild type mice, menthol (100 and 200 $\mu$M) did not have an effect on the drug induced locomotor rhythm (Fig. 7B, 7C, 7D, $n=4$). There was no significant change in the stability (PTCC: L2–L5, $P>0.5$; AC max: L2, $P>0.1$, L5, $P>0.1$) or phase of the rhythm (modified Rayleigh's, $P<0.05$; Watson–Williams, $P>0.5$). Overall, these data show that menthol-induced modulation of drug-induced rhythmicity is mediated by activation of TRPM8 (Fig. 7E).

### Effects on synaptic transmission during TRPV1 mediated modulation of CPG

We investigated probable mechanisms by which capsaicin (TRPV1) or menthol (TRPM8) modulated the CPG. The modulation of central sensitization in pain models mediated by TRPV1 and TRPM8 involves glutamatergic synaptic transmission mechanisms between C and A$\delta$ terminals and second order neurons in the dorsal horn of the spinal cord (Willis, 2001; Baccei et al., 2003; Proudfoot et al., 2006). These synapses are subject to further modulation by descending pathways projecting from higher centers (Millan, 2002). Capsaicin is known to activate TRPV1 and mediate excitatory glutamatergic neurotransmission by NMDAR mechanisms that potentially involve AMPAR activation (Fig. 8E) (Willis, 2001). Antagonists of NMDAR (APV: 50-100 $\mu$M) and AMPAR (CNQX: 10–40 $\mu$M) were used to investigate whether capsaicin-mediated excitatory glutamatergic synaptic transmission modulates CPG activity.

To target the glutamatergic mechanisms, we turned to a purely excitatory network where inhibitory synaptic transmission was blocked using a combination of the glycine receptor antagonist strychnine (2 $\mu$M), $GABA_A$ antagonist picrotoxin (50 $\mu$M) and $GABA_B$ antagonist CGP (50 $\mu$M). This rhythm is characterized by slow synchronous bursts representing a disinhibited rhythm (Bracci et al., 1996; Giuliano Taccola, 2004). Once a stable synchronous rhythm developed, capsaicin (1 $\mu$M) was bath-applied to the whole cord. An initial increase followed by a decrease in the frequency of rhythmic bursts was observed following bath application of capsaicin (Fig. 8A, $n$=4). The effect of capsaicin was not blocked in the presence APV (50–100 $\mu$M) (Fig. 8B, $n$=4) or CNQX (10–40 $\mu$M) (Fig. 8C, $n$=4). However, the capsaicin-induced modulation of the CPG was completely blocked by bath-applying both APV (100 $\mu$M) and CNQX (40 $\mu$M) (Fig. 8D, $n$=4). Again, capsaicin-induced modulation was not observed in spinal cord preparations from *trpv1*$^{-/-}$ mice (data not shown). These results suggest that capsaicin promotes excitatory glutamatergic neurotransmission via NMDAR and/or AMPAR following activation of capsaicin-sensitive TRPV1 expressing C and A$\delta$ projections onto the lumbar segments, which in turn modulates the CPG (Fig. 8E).

### Effects on synaptic transmission during TRPM8-mediated modulation of the CPG

TRPM8-mediated mechanisms were investigated using the disinhibited rhythm evoked by blocking fast synaptic transmission (as described in the previous section). It has been reported that TRPM8 produces its analgesic action through activation of inhibitory glutamatergic mGluR type II and III mechanisms (Proudfoot et al., 2006). We hypothesized that TRPM8 actions on spinal motor networks were mediated by similar mechanisms (Fig. 9C).

A stable synchronous rhythm was obtained by blocking inhibitory transmission using a combination of the strychnine (2 $\mu$M), picrotoxin (50 $\mu$M) and CGP (50 $\mu$M) applied to the whole cord (T5–cauda equina) (Fig. 9Ai, 9Bi, $n$=6). Once a stable synchronous rhythm developed, menthol (100 and 200 $\mu$M) was bath-applied to the whole cord and resulted in a complete blockade of the rhythm (Fig. 9Aii–iii, $n$=6). We could reverse this blockade by applying mGluR II and III antagonists LY341495 (50 $\mu$M) and UBP1112 (50 $\mu$M), respectively (Fig. 9Aiv, $n$=6). We found that this was also true if we added the antagonists before bath applying menthol (Fig. 9Bii–iv, $n$=6). Menthol-induced modulation of the synchronous rhythm was not observed in spinal cord preparations from *trpm8*$^{-/-}$ mice (data not shown). These results suggest that menthol promotes inhibitory glutamatergic neurotransmission via mGluR II/III receptors following activation of menthol-sensitive dorsal horn TRPM8 positive afferents (although, a role for ventral midline TRPM8 cannot be ruled out), which in turn modulates the CPG (Fig. 9C).

### Capsaicin or menthol modulation of motor function does not occur by direct action on motoneurons

To verify whether capsaicin or menthol was modulating the motor output by a direct action on motoneurons, we used whole-cell patch clamp techniques to examine intrinsic motoneuron electrical properties. Bath-application of capsaicin (1 $\mu$M) or menthol (100 or 200 $\mu$M) had no significant effect on any of the properties measured (Tables 1 and 2, $n$=8 for capsaicin, $n$=9 for 100 $\mu$M menthol and $n$=10 for 200 $\mu$M menthol). We monitored input resistance every 2 s before and during administration of capsaicin. There was no significant effect of capsaicin on input resistance (Suppl. Fig. 3). The resting potential was the same before and after the administration of capsaicin without changing the holding current. After achieving the whole-cell configuration the motoneurons were held at −70 mV (corrected for the junction potential, see Experimental Procedures). There was no spontaneous action potential activity at the −70 mV holding potential.

### Peripheral activation of TRPV1 and TRPM8 modulates drug-evoked locomotor rhythms

We tested the possible modulation of locomotor rhythms by peripheral activation of TRPV1 and TRPM8 in wild type, *trpv1*$^{-/-}$ and *trpm8*$^{-/-}$ mice (Fig. 10C). These studies used hind limb attached spinal cord preparations that had their spinal cords transected at T5 and their ventral roots cut. The lumbosacral dorsal roots from the hind limb were not cut. A split-bath was built with Vaseline walls to separate the spinal cord portion from the hind limb. Rhythmic motor activity was evoked by bath application of NMA (5 $\mu$M), 5-HT (10 $\mu$M), and DA (50 $\mu$M) to the spinal cord compartment (Fig. 10Ai, 10Bi). Once a stable rhythm was achieved, we injected capsaicin (1 $\mu$M) intradermally into the hind limb. Within 5 min of the capsaicin injection, the cycle period decreased (Fig. 10Aii, 10Biv, $n$=4). Capsaicin application did not change the burst amplitude ($P$>0.5) or phase (modified Rayleigh's, $P$<0.05; Watson–Williams, $P$>0.05). There was no change in any recorded parameters in the *trpv1*$^{-/-}$ preparations following injection of capsaicin (Fig. 10Aiii, $n$=3). A more physiological stimuli such as thermal activation of the hind paw by heat (Caterina et al., 1997) was not used to eliminate possible activation of other heat-sensitive TRPs such as TRPV3 and TRPV4 during application of a heat ramp (~32 to ~45 °C) (Lumpkin, 2007). However, we were able to use the physiological thermal activation of hind paw by cooling (~32 to ~17 °C) which lacked such a caveat. Following cooling of the hind paw, a significant increase in the cycle period was observed in wild type but not *trpm8*$^{-/-}$ mice (Fig. 10Bii, 10Biv, $n$=3). In the wild type preparations, following rewarming of the hind paw to control temperatures ~32 °C, the rhythm frequency returned to control values (Fig. 10Biii, 10Biv). These results suggested that peripheral activation of TRPM8 by cooling can also modulate locomotor rhythm. However, unlike activation of spinal cord TRPM8 by bath application of menthol, peripheral activation of TRPM8 by cooling did not decrease the burst amplitude of the rhythm ($P$>0.5). Cooling did not change the phase (modified Rayleigh's, $P$<0.01; Watson–Williams, $P$>0.5) in wild type or *trpm8*$^{-/-}$ preparations. We did not use intra-dermal applications of menthol since the high concentrations required may have nonspecific effects on TRPV3 and TRPA1 in the skin (Macpherson et al., 2006;Lumpkin, 2007). Icilin, which is a potent agonist of TRPM8 (Macpherson et al., 2006), was not applied as we found it had nonspecific effects when used on isolated spinal cord preparations.

## Discussion

The goal of this study was to identify the role of distinct somatosensory and nociceptive afferents in the control of locomotion and to describe a set of tools to effectively do so using isolated spinal cord preparations. To accomplish this, we focused on the modulation of thermoTRPs, which underlie the transduction of hot and cold sensation in the skin (Venkatachalam and Montell, 2007). These receptors are located both in the peripheral and central terminals of afferents (Julius and Basbaum, 2001; Levine and Alessandri-Haber,

2007; Willis, 2007). We chose to investigate spinal projections of nociceptive afferent subsets that express TRPV1 or TRPM8, both of which are known to modulate central sensitization in nociceptive pathways (Willis, 2001, 2007; Fleetwood-Walker et al., 2007; Nilius and Voets, 2007; Spicarova and Palecek, 2008). Several lines of evidence drawn from our work suggest that spinal TRPV1 and TRPM8 afferent terminals contribute to the modulation of spinal locomotor networks (CPG) responsible for generating the locomotor pattern.

### Capsaicin and noxious heat sensing afferents (TRPV1)

Bath application of capsaicin was able to transiently increase the frequency of the drug-evoked locomotor rhythm. This effect was distributed throughout the thoracolumbosacral spinal cord, suggesting that TRPV1 afferent fibers contributing to CPG modulation were not restricted to any one segment. This was confirmed by our data showing that TRPV1 was expressed in lumbosacral segments. The transient increase in the frequency of the drug-evoked fictive locomotor rhythm is typical of a capsaicin-sensitive sensitization and desensitization mechanism that has been demonstrated to be TRPV1 dependent, and which we confirmed using *trpv1*$^{-/-}$ mice. The sensitization and desensitization effects were also observed when locomotion was evoked following electrical stimulation of afferents. However, in these cases the rhythmic discharges became tonic and then completely silent representing the sensitization and desensitization effects of capsaicin, respectively on TRPV1 positive afferents. If activation of TRPV1 were occurring at sites different from the stimulated afferents, then one would expect a transient increase in frequency similar to what we observed for non-afferent stimulation. Surprisingly, when capsaicin was applied to thoracolumbar segments (rostral to the L6/S1 split bath) during stimulation of S4 dorsal roots, we found that after 10 minutes the stimulus was no longer able to evoke a rhythmic pattern. We expected to see that the rhythm would be transiently affected and not blocked. The most likely explanation for these effects is that a subpopulation of TRPV1 afferents projects beyond the L6/S1 Vaseline dam through the dorsal tract of Lissauer. In the rat, A$\delta$ nociceptive afferent collaterals can extend up to seven segments via the tract of Lissauer (Lidierth, 2007). The afferent terminals rostral to the split would be desensitized by capsaicin, thereby blocking the stimulus evoked rhythm. It is possible that the rostral TRPV1 afferents project onto the VLF. However, other pathways could be involved and our data cannot discriminate between the two possibilities. The major distinction between the capsaicin effects in electrical- versus drug-evoked fictive locomotion in the isolated en bloc spinal cord is in the elements that drive rhythmic activity. During the electrically-evoked fictive locomotion, capsaicin sensitizes and silences nociceptive afferents suggested here to be sufficient but not essential elements in activating the locomotor CPG. On the other hand, during drug-evoked fictive locomotion, rhythmogenic drugs provide the drive to activate the CPG and we suggest that the capsaicin effects are on the nociceptive afferents that then lead to downstream modulation of the network.

The increase in drug-evoked fictive locomotor frequency was seen upon both central activation of TRPV1 in isolated en bloc spinal cord and peripheral activation of TRPV1 afferent endings in our leg attached-spinal cord preparation. Evidence from previous work on pain mechanisms suggests that this excitatory mechanism is based on increased release of glutamate from TRPV1 positive afferent terminals that activate AMPA and NMDA receptors (Willis, 2001). We were able to confirm a similar effect of TRPV1 on network function, by making use of a disinhibited evoked rhythm (Bracci et al., 1996) following blockade of $GABA_{A,\ B}$ and glycine receptors. The disinhibited rhythm model allowed us to address whether excitatory glutamatergic mechanisms were activated by capsaicin's action on TRPV1 positive afferent terminals. Capsaicin's action on the disinhibited rhythm was completely blocked in the presence of NMDA and AMPA receptor antagonists, suggesting that activation of excitatory glutamatergic mechanisms occurs by way of these receptors. We did not observe any effect of capsaicin on the disinhibited rhythm in preparations from *trpv1*$^{-/-}$, confirming the role for TRPV1. Since

TRPV1 is expressed in heat-sensitive receptors (Caterina et al., 1997), and in the central projections of these afferents, it strongly argues that the effects on the CPG are mediated primarily by actions of capsaicin on TRPV1 afferent terminals. We observed that TRPV1 expression was restricted to the superficial dorsal horn in neonatal spinal cord compared to a more distributed expression in the adult which includes deeper dorsal horn and some projections reaching ventral horn laminae (Tominaga et al., 1998; Spicarova and Palecek, 2008). Consistent with our immunohistochemical data, we found no evidence that capsaicin affected intrinsic motoneuronal properties and there was no TRPV1 expression on the ventral horn. Taken together, these data provide additional evidence that TRPV1 acts on the afferent terminal in the thoracolumbosacral dorsal horn thereby modulating downstream motor networks.

### Menthol and cold sensing afferents (TRPM8)

While TRPV1 had a general excitatory effect followed by desensitization, TRPM8 activation displayed an attenuation of network activity that was sustained. Work from several laboratories suggests that TRPM8 are expressed on unmyelinated afferents that are responsive to menthol or cool temperatures and possibly some nociceptive afferents. Our work has shown that the TRPM8 agonist menthol depressed network activity, an effect that was reversed when mGluR type II and III receptors were blocked. An analgesic action of menthol has been observed in models of neuropathic pain acting through similar mechanisms. Proudfoot and colleagues (2006) suggest that TRPM8 increases the release of glutamate that in turn activates mGluR type II and III receptors that are expressed presynaptically on neighboring terminals. Our data indicate that this mechanism may be operational at sacral segments where TRPM8 is clearly expressed in the dorsal horn. Our work suggests that the menthol-sensitive TRPM8 afferents or their projections do not contribute synaptic inputs onto VLF interneurons along the SCA pathway. This is because application of menthol within sacral regions had no effect on the frequency of locomotor activity. This does not imply that TRPM8 is without effect within sacral segments. First, data presented here show clear expression of TRPM8 within the dorsal horn of the sacral cord. Second, electrophysiological evidence suggests that TRPM8 modulates the windup response within sacral segments (Mandadi and Whelan, unpublished observations). To our surprise, the major effects of menthol on SCA-induced locomotor activity occurred only when menthol was applied to the thoracolumbar compartment. We have two explanations for these effects. First, our data show that TRPM8 is expressed on cells located at the midline of the ventral horn. At the moment we have no data on the identity of these cells or their projections, except that they do not appear to be Hb9 cells, thought to contribute to rhythmic activity (Wilson et al., 2005). However, an earlier study showed evidence for modulation of motor rhythm by mGluR II/III that occurred at the CPG network level (Taccola et al., 2003). Thus, the activation of network level mGluR II/III mechanisms by menthol via the ventral horn expression of TRPM8 close to putative CPG networks cannot be ruled out. Such activation of TRPM8 ion channels expressed postsynaptically may be restricted to the neonatal stage of development since adult expression is restricted to the dorsal horn (Takashima et al., 2007; Dhaka et al., 2008). Another possibility is that menthol reduces spontaneous release of glutamate from central afferent terminals by an indirect action mediated through group II/III mGluRs (Proudfoot et al., 2006). Consistent with this idea we found clear TRPM8 expression in lamina I/II. Also, supporting the idea of direct effects on central afferent terminals, is the fact that peripheral activation of TRPM8 in skin by cooling resulted in a slowing of the rhythm similar to what we observed when we applied menthol to the thoracolumbar spinal cord.

### Endogenous ligands

The endogenous ligands for TRPM8 and TRPV1 have not been conclusively found, however several possible candidates have been suggested. Chronic pain mechanisms within the spinal cord may involve activation of intracellular phospholipase-A2 (PLA2) pathways (Lucas et al.,

2005). Activation of PLA2 results in enzyme hydrolysis of cell membrane phospholipids to produce arachidonic acid (AA) (Kita, 2006) and lyso-phospholipids (LysoPL) (Balsinde and Balboa, 2005) which have been shown to activate TRPV1 and TRPM8, respectively (Hwang et al., 2000; Shin et al., 2002; Abeele et al., 2006; Andersson et al., 2007). For TRPV1, candidate endogenous ligands also include metabolites of AA (Hwang et al., 2000) and the endocannabinoids such as anandamide (Zygmunt et al., 1999). Of these, AA and LysoPL produce proinflammatory mediator eicosanoids (Yedgar et al., 2006), whereas anandamide has anti-nociceptive properties attributable to activation of cannabinoid receptors (Benjamin and Cravatt, 2004). Also, under certain circumstances, anti-inflammatory actions of LysoPL may be attributable to its ability to activate TRPM8. It would be interesting to dissect out if these endogenous ligands of TRPV1 or TRPM8 mimic effects of capsaicin or menthol, respectively. However, the PLA2 pathways or endogenous ligands generated are not specific to TRPV1 or TRPM8 and may have multiple targets. Our study thus provides novel insights into more upstream receptor-level–mediated spinal mechanisms specific to TRPV1 or TRPM8. Such mechanisms operating between pain and locomotor networks present an interesting scenario for the involvement of endogenous ligands.

## Relationship to FRA system

We found that locomotion could still be elicited in TRPM8 and TRPV1 knockout mice indicating that these classes of afferents were not necessary for the afferent evoked locomotion seen here. Furthermore, following desensitization of TRPV1 afferents and loss of network output, higher stimulus intensities (≥8 T) applied to the same dorsal root could reactivate networks. Overall our data led us to hypothesize that many different reflex pathways contribute to locomotion beyond the ones identified here. These additional subclasses could include proprioceptors (Rossignol et al., 2006) and other high threshold nociceptors not sensitive to capsaicin or menthol (Caterina et al., 2000; Bautista et al., 2007). One caveat is that at higher stimulus intensities (≥8 T) subpopulations of TRPV1 positive afferents that were not desensitized at the initial dose of capsaicin (1 $\mu$M) may have been recruited. Nevertheless, it is interesting to speculate that what we are observing here is a correlate of the FRA system that has been described in cats (Duysens and Pearson, 1976; Lundberg, 1979; Conway et al., 1988; Gossard et al., 1994; Lam and Pearson, 2002). Classically, FRA systems consist of input from a wide range of modalities onto common sets of interneurons resulting in a defined behavioral output. There are generally two types of reflex responses associated with the FRA system: short-latency FRA pathways which when activated generally result in flexion responses in the ipsilateral limbs and extension in the contralateral limbs, and so-called long-latency FRA pathways which are released following addition of L-DOPA in cat preparation (Jankowska et al., 1967a,b; Lundberg, 1979). Stimulation of high-threshold afferents with trains of stimuli in the presence of L-DOPA has been shown to elicit short bursts of alternating activity from flexors and extensors (Lundberg, 1979; Schomburg et al., 1998). Lundberg concluded that these patterns suggested that FRA could access the CPG. Nociceptive input has been shown to contribute, at least in part, to the FRA system (Schomburg et al., 1998). For example, noxious heat can facilitate rhythmic activity in acute spinal cats (Schomburg et al., 2001). Work by Lev-Tov and colleagues (Blivis et al., 2007) has established that noxious heat delivered to the skin can elicit bouts of locomotor activity in tail-attached spinal cord preparations. It is tempting to consider that some of the TRPM8 and TRPV1 afferents project onto FRA interneurons. While much work will be required to test this hypothesis, the use of genetic tools holds much promise for future work in this area (Gordon and Whelan, 2006). For example, it should be possible to use mice where subclasses of interneurons are identified in combination with expression of TRPM8 and TRPV1. These types of tools would be a starting point for identifying the intercalated interneurons in the reflex pathways that modulate nociceptive feedback onto CPG networks.

**APPENDIX:** Supplementary data: Supplementary data associated with this article can be found, in the online version, at doi: 10.1016/j.neuroscience.2009.05.063.

## Supplementary Material

Refer to Web version on PubMed Central for supplementary material.

## Acknowledgments

We would like to thank Michelle Tran for her excellent technical assistance. We greatly appreciate ongoing support from the Alberta Heritage Foundation for Medical Research, the Canadian Institutes of Health Research, and the University of Calgary. Dr. Sravan Mandadi was supported by a fellowship from the Alberta Heritage Foundation for Medical Research. Dr. Stan Nakanishi was supported by a fellowship from the Hotchkiss Brain Institute.

## References

Abeele FV, Zholos A, Bidaux G, Shuba Y, Thebault S, Beck B, Flourakis M, Panchin Y, Skryma R, Prevarskaya N. $Ca^{2+}$-independent phospholipase A2-dependent gating of TRPM8 by lysophospholipids. J Biol Chem 2006;281:40174–40182. [PubMed: 17082190]

Andersson DA, Nash M, Bevan S. Modulation of the cold-activated channel TRPM8 by lysophospholipids and polyunsaturated fatty acids. J Neurosci 2007;27:3347–3355. [PubMed: 17376995]

Arber S, Han B, Mendelsohn M, Smith M, Jessell TM, Sockanathan S. Requirement for the homeobox gene Hb9 in the consolidation of motor neuron identity. Neuron 1999;23:659–674. [PubMed: 10482234]

Baccei ML, Bardoni R, Fitzgerald M. Development of nociceptive synaptic inputs to the neonatal rat dorsal horn: glutamate release by capsaicin and menthol. J Physiol 2003;549:231–242. [PubMed: 12679376]

Balsinde J, Balboa MA. Cellular regulation and proposed biological functions of group VIA calcium-independent phospholipase A2 in activated cells. Cell Signal 2005;17:1052–1062. [PubMed: 15993747]

Barthélemy D, Leblond H, Rossignol S. Characteristics and mechanisms of locomotion induced by intraspinal microstimulation and dorsal root stimulation in spinal cats. J Neurophysiol 2007;97:1986–2000. [PubMed: 17215509]

Bautista DM, Siemens J, Glazer JM, Tsuruda PR, Basbaum AI, Stucky CL, Jordt SE, Julius D. The menthol receptor TRPM8 is the principal detector of environmental cold. Nature 2007;448:204–208. [PubMed: 17538622]

Benjamin F, Cravatt AHL. The endogenous cannabinoid system and its role in nociceptive behavior. J Neurobiol 2004;61:149–160. [PubMed: 15362158]

Bertrand S, Cazalets JR. The respective contribution of lumbar segments to the generation of locomotion in the isolated spinal cord of newborn rat. Eur J Neurosci 2002;16:1741–1750. [PubMed: 12431227]

Blivis D, Mentis GZ, O'Donovan MJ, Lev-Tov A. Differential effects of opioids on sacrocaudal afferent pathways and central pattern generators in the neonatal rat spinal cord. J Neurophysiol 2007;97:2875–2886. [PubMed: 17287435]

Bracci E, Ballerini L, Nistri A. Spontaneous rhythmic bursts induced by pharmacological block of inhibition in lumbar motoneurons of the neonatal rat spinal cord. J Neurophysiol 1996;75:640–647. [PubMed: 8714641]

Caterina MJ, Schumacher MA, Tominaga M, Rosen TA, Levine JD, Julius D. The capsaicin receptor: a heat-activated ion channel in the pain pathway. Nature 1997;389:816–824. [PubMed: 9349813]

Caterina MJ, Leffler A, Malmberg AB, Martin WJ, Trafton J, Petersen-Zeitz KR, Koltzenburg M, Basbaum AI, Julius D. Impaired nociception and pain sensation in mice lacking the capsaicin receptor. Science 2000;288:306–313. [PubMed: 10764638]

Clapham DE, Julius D, Montell C, Schultz G. International Union of Pharmacology. XLIX. Nomenclature and structure-function relationships of transient receptor potential channels. Pharmacol Rev 2005;57:427–450. [PubMed: 16382100]

Conway BA, Hultborn H, Kiehn O, Mintz I. Plateau potentials in alpha-motoneurones induced by intravenous injection of L-dopa and clonidine in the spinal cat. J Physiol 1988;405:369–384. [PubMed: 3255795]

Dhaka A, Earley TJ, Watson J, Patapoutian A. Visualizing cold spots: TRPM8-expressing sensory neurons and their projections. J Neurosci 2008;28:566–575. [PubMed: 18199758]

Dhaka A, Murray AN, Mathur J, Earley TJ, Petrus MJ, Patapoutian A. TRPM8 is required for cold sensation in mice. Neuron 2007;54:371–378. [PubMed: 17481391]

Duysens J, Pearson KG. The role of cutaneous afferents from the distal hindlimb in the regulation of the step cycle of thalamic cats. Exp Brain Res 1976;24:245–255. [PubMed: 1253857]

Eccles RM, Lundberg A. Synaptic actions in motoneurones by afferents which may evoke the flexion reflex. Arch Ital Biol 1959;97:199–221.

Fleetwood-Walker SM, Proudfoot CWJ, Garry EM, Allchorne A, Vinuela-Fernandez I, Mitchell R. Cold comfort. Pharm Trends Pharmacol Sci 2007;28:621–628.

Giuliano T, Cristina M, Andrea N. Role of group II and III metabotropic glutamate receptors in rhythmic patterns of the neonatal rat spinal cord in vitro. Exp Brain Res 2004;156:495–504. [PubMed: 15007577]

Gordon IT, Whelan PJ. Deciphering the organization and modulation of spinal locomotor central pattern generators. J Exp Biol 2006;209:2007–2014. [PubMed: 16709903]

Gossard JP, Floeter MK, Kawai Y, Burke RE, Chang T, Schiff SJ. Fluctuations of excitability in the monosynaptic reflex pathway to lumbar motoneurons in the cat. J Neurophysiol 1994;72:1227–1239. [PubMed: 7807207]

Han P, Nakanishi S, Tran M, Whelan PJ. Dopaminergic modulation of spinal neuronal excitability. J Neurosci 2007;27:13192–13204. [PubMed: 18045913]

Hinckley CA, Hartley R, Wu L, Todd A, Ziskind-Conhaim L. Locomotor-like rhythms in a genetically distinct cluster of interneurons in the mammalian spinal cord. J Neurophysiol 2005;93:1439–1449. [PubMed: 15496486]

Hwang SW, Cho H, Kwak J, Lee SY, Kang CJ, Jung J, Cho S, Min KH, Suh YG, Kim D, Oh U. Direct activation of capsaicin receptors by products of lipoxygenases: endogenous capsaicin-like substances. Proc Natl Acad Sci U S A 2000;97:6155–6160. [PubMed: 10823958]

Jankowska E, Jukes MG, Lund S, Lundberg A. The effect of DOPA on the spinal cord. 6. Half-centre organization of interneurones transmitting effects from the flexor reflex afferents. Acta Physiol Scand 1967a;70:389–402. [PubMed: 4294400]

Jankowska E, Jukes MG, Lund S, Lundberg A. The effect of DOPA on the spinal cord. 5. Reciprocal organization of pathways transmitting excitatory action to alpha motoneurones of flexors and extensors. Acta Physiol Scand 1967b;70:369–388. [PubMed: 4293473]

Jiang Z, Carlin KP, Brownstone RM. An in vitro functionally mature mouse spinal cord preparation for the study of spinal motor networks. Brain Res 1999;816:493–499. [PubMed: 9878874]

Julius D, Basbaum AI. Molecular mechanisms of nociception. Nature 2001;413:203–210. [PubMed: 11557989]

Kita Y, Uozumi N, Shimizu T. Biochemical properties and pathophysiological roles of cytosolic phospholipase A(2)s. Biochim Biophys Acta 2006;1761:1317–1322. [PubMed: 16962823]

Kjaerulff O, Kiehn O. Distribution of networks generating and coordinating locomotor activity in the neonatal rat spinal cord in vitro: a lesion study. J Neurosci 1996;16:5777–5794. [PubMed: 8795632]

Lam T, Pearson KG. The role of proprioceptive feedback in the regulation and adaptation of locomotor activity. Adv Exp Med Biol 2002;508:343–355. [PubMed: 12171130]

Lev-Tov A, Delvolve I, Kremer E. Sacrocaudal afferents induce rhythmic efferent bursting in isolated spinal cords of neonatal rats. J Neurophysiol 2000;83:888–894. [PubMed: 10669502]

Levine JD, Alessandri-Haber N. TRP channels: targets for the relief of pain. Biochim Biophys Acta 2007;1772:989–1003. [PubMed: 17321113]

Lidierth M. Long-range projections of Adelta primary afferents in the Lissauer's tract of the rat. Neurosci Lett 2007;425:126–130. [PubMed: 17850967]

Lucas KK, Svensson CI, Hua XY, Yaksh TL, Dennis EA. Spinal phospholipase A2 in inflammatory hyperalgesia: role of group IVA cPLA2. Br J Pharmacol 2005;144:940–952. [PubMed: 15685208]

Lumpkin EA, C M. Mechanisms of sensory transduction in the skin. Nature 2007;445:858–865. [PubMed: 17314972]

Lundberg A. Multisensory control of spinal reflex pathways. Prog Brain Res 1979;50:11–28. [PubMed: 121776]

Macpherson LJ, H S, Miyamoto T, Dubin AE, Patapoutian A, Story GM. More than cool: promiscuous relationships of menthol and other sensory compounds. Mol Cell Neurosci 2006;32:335–343. [PubMed: 16829128]

Mandadi, S.; Nakanishi, ST.; Takashima, Y.; McKemy, DD.; Dhaka, A.; Patapoutian, A.; Whelan, P. Society for Neuroscience. 2008. TRPV1 and TRPM8 can control movement by modulating sensorimotor pathways within the spinal cord. 375.18/OO17

Mandadi, S.; Whelan, P. Society for Neuroscience. Vol. 37. 2007. Modulation of windup and fictive locomotion in isolated mouse spinal cord by TRP channels; p. 78.16

McKemy DD, Neuhausser WM, Julius D. Identification of a cold receptor reveals a general role for TRP channels in thermosensation. Nature 2002;416:52–58. [PubMed: 11882888]

Millan MJ. Descending control of pain. Prog Neurobiol 2002;66:355–474. [PubMed: 12034378]

Nilius B. TRP channels in disease. Biochim Biophys Acta 2007;1772:805–812. [PubMed: 17368864]

Nilius B, Voets T. Neurophysiology: channelling cold reception. Nature 2007;448:147–148. [PubMed: 17625555]

Nilius B, Owsianik G, Voets T, Peters JA. Transient receptor potential cation channels in disease. Physiol Rev 2007;87:165–217. [PubMed: 17237345]

Pearson KG. Generating the walking gait: role of sensory feedback. Prog Brain Res 2004;143:123–129. [PubMed: 14653157]

Pearson SA, Mouihate A, Pittman QJ, Whelan PJ. Peptidergic activation of locomotor pattern generators in the neonatal spinal cord. J Neurosci 2003;23:10154–10163. [PubMed: 14602832]

Peier AM, Moqrich A, Hergarden AC, Reeve AJ, Andersson DA, Story GM, Earley TJ, Dragoni I, McIntyre P, Bevan S, Patapoutian A. A TRP channel that senses cold stimuli and menthol. Cell 2002;108:705–715. [PubMed: 11893340]

Proudfoot CJ, Garry EM, Cottrell DF, Rosie R, Anderson H, Robertson DC, Fleetwood-Walker SM, Mitchell R. Analgesia mediated by the TRPM8 cold receptor in chronic neuropathic pain. Curr Biol 2006;16:1591–1605. [PubMed: 16920620]

Rossignol S, Dubuc R, Gossard JP. Dynamic sensorimotor interactions in locomotion. Physiol Rev 2006;86:89–154. [PubMed: 16371596]

Schomburg E, Steffens H, Wada N. Parallel nociceptive reflex pathways with negative and positive feedback functions to foot extensors in the cat. J Physiol 2001;536:605–613. [PubMed: 11600693]

Schomburg ED, Petersen N, Barajon I, Hultborn H. Flexor reflex afferents reset the step cycle during fictive locomotion in the cat. Exp Brain Res 1998;122:339–350. [PubMed: 9808307]

Shin J, Cho H, Hwang SW, Jung J, Shin CY, Lee SY, Kim SH, Lee MG, Choi YH, Kim J, Haber NA, Reichling DB, Khasar S, Levine JD, Oh U. Bradykinin-12-lipoxygenase-VR1 signaling pathway for inflammatory hyperalgesia. Proc Natl Acad Sci U S A 2002;99:10150–10155. [PubMed: 12097645]

Spicarova D, Palecek J. The role of spinal cord vanilloid (TRPV1) receptors in pain modulation. Physiol Res 2008;57:S69–S77. [PubMed: 18481913]

Strauss I, Lev-Tov A. Neural pathways between sacrocaudal afferents and lumbar pattern generators in neonatal rats. J Neurophysiol 2003;89:773–784. [PubMed: 12574455]

Szolcsányi J. Forty years in capsaicin research for sensory pharmacology and physiology. Neuropeptides 2004;38:377–384. [PubMed: 15567473]

Taccola G, Marchetti C, Nistri A. Effect of metabotropic glutamate receptor activity on rhythmic discharges of the neonatal rat spinal cord in vitro. Exp Brain Res 2003;153:388–393. [PubMed: 14523604]

Takashima Y, Daniels RL, Knowlton W, Teng J, Liman ER, McKemy DD. Diversity in the neural circuitry of cold sensing revealed by genetic axonal labeling of transient receptor potential melastatin 8 neurons. J Neurosci 2007;27:14147–14157. [PubMed: 18094254]

Thaler J, Harrison K, Sharma K, Lettieri K, Kehrl J, Pfaff SL. Active suppression of interneuron programs within developing motor neurons revealed by analysis of homeodomain factor HB9. Neuron 1999;23:675–687. [PubMed: 10482235]

Tominaga M, Tominaga T. Structure and function of TRPV1. Pflügers Arch 2005;451:143–150.

Tominaga M, Caterina MJ, Malmberg AB, Rosen TA, Gilbert H, Skinner K, Raumann BE, Basbaum AI, Julius D. The cloned capsaicin receptor integrates multiple pain-producing stimuli. Neuron 1998;21:531–543. [PubMed: 9768840]

Venkatachalam K, Montell C. TRP channels. Annu Rev Biochem 2007;76:387–417. [PubMed: 17579562]

Watson GS, Williams EJ. On the construction of significance tests on the circle and the sphere. Biometrica 1956;43:344–352.

Whelan P, Bonnot A, O'Donovan MJ. Properties of rhythmic activity generated by the isolated spinal cord of the neonatal mouse. J Neurophysiol 2000;84:2821–2833. [PubMed: 11110812]

Willis WD Jr. The somatosensory system, with emphasis on structures important for pain. Brain Res Rev 2007;55:297–313. [PubMed: 17604109]

Willis WD Jr. Role of neurotransmitters in sensitization of pain responses. Ann N Y Acad Sci 2001;933:142–156. [PubMed: 12000017]

Wilson JM, Hartley R, Maxwell DJ, Todd AJ, Lieberam I, Kaltschmidt JA, Yoshida Y, Jessell TM, Brownstone RM. Conditional rhythmicity of ventral spinal interneurons defined by expression of the Hb9 homeodomain protein. J Neurosci 2005;25:5710–5719. [PubMed: 15958737]

Yedgar S, Cohen Y, Shoseyov D. Control of phospholipase A2 activities for the treatment of inflammatory conditions. Biochim Biophys Acta 2006;1761:1373–1382. [PubMed: 16978919]

Zar, JH. Biostatistical analysis. 4th. Upper Saddle River, NJ: Prentice Hall; 1999.

Zygmunt PM, Petersson J, Andersson DA, Chuang HH, Sorgard M, Di Marzo V, Julius D, Hogestatt ED. Vanilloid receptors on sensory nerves mediate the vasodilator action of anandamide. Nature 1999;400:452–457. [PubMed: 10440374]

## Abbreviations

| | |
|---|---|
| AA | arachidonic acid |
| ACSF | artificial cerebrospinal fluid |
| AMPAR | AMPA receptors |
| CPG | central pattern generator |
| DA | dopamine |
| FRA | flexor reflex afferents |
| Hb9 | homeobox gene 9 |
| LysoPL | lyso-phospholipid |
| L2 | lumbar segment 2 |
| L5 | lumbar segment 5 |
| L6 | lumbar segment 6 |
| mGluR | metabotropic glutamate receptors |
| NMA | *N*-methyl-$_{D}$($_{L}$)-aspartic acid |
| NMDAR | *N*-methyl-$_{D}$-aspartic acid receptors |
| P | postnatal day zero |
| PBS+ TX | PBS plus 0.1% Triton X-100 |
| PLA2 | phospholipase-A2 |

| | |
|---|---|
| PTCC | peak-to-trough correlation coefficient |
| SCA | sacrocaudal afferents |
| S1 | sacral segment 1 |
| S4 | sacral segment 4 |
| T | stimulus threshold |
| TRP | transient receptor potential |
| TRPM8 | transient receptor potential melastatin 8 |
| *trpm8*$^{-/-}$ | transient receptor potential melastatin 8-null mice |
| TRPV1 | transient receptor potential vanilloid 1 |
| *trpv1*$^{-/-}$ | transient receptor potential vanilloid 1-null mice |
| T5 | thoracic segment 5 |
| VLF | ventrolateral funiculus |

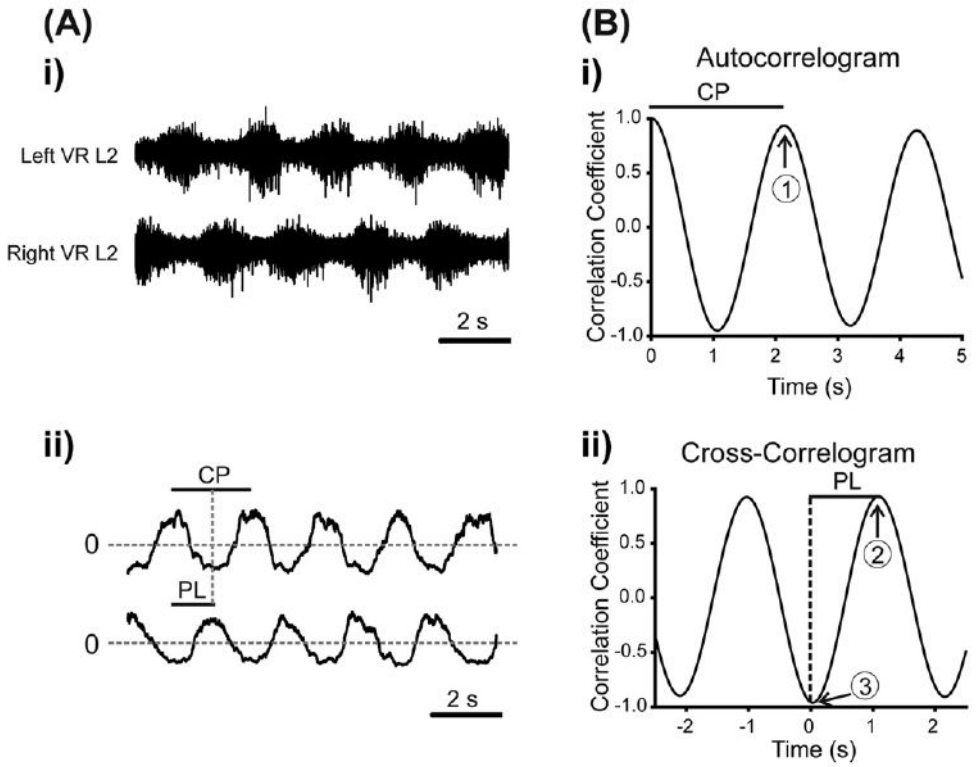


**Fig. 1.**

Time series analyses techniques for calculating rhythm parameters. (A) (i) Raw data showing a sequence of rhythmic data from the L2 ventral root neurograms. (A) (ii) The mean of each neurogram trace was calculated and subtracted and the absolute value was then obtained, so that each neurogram oscillated around zero. (B) (i) The autocorrelograms for each neurogram were then obtained (only data from the Left L2 trace are displayed for clarity). The cycle period (CP in diagram) for the resultant rhythm was calculated by measuring the number of lags from 0 to the first peak in the autocorrelogram; this is marked by the number 1 in the trace. These values were then converted back to time in seconds. To provide a measure of the quality of the rhythm for each neurogram, we calculated the absolute value of this next peak (termed autocorrelation (AC) max). (B) (ii) The phase lag (PL) between ventral root bursts was obtained from the cross-correlogram and was defined as the number of lags from lag 0 to the next positive peak (3 in diagram), converted to seconds, and divided by the cycle period (1 in Bi). Finally, taking the difference between the minimum and maximum peaks (3–2 in the diagram) of the cross-correlogram and expressing this as an absolute value was used to determine the stability of the coupling between the rhythm produced by the left and right L2 ventral roots (termed PTCC). The maximum value would be 2 in this case.

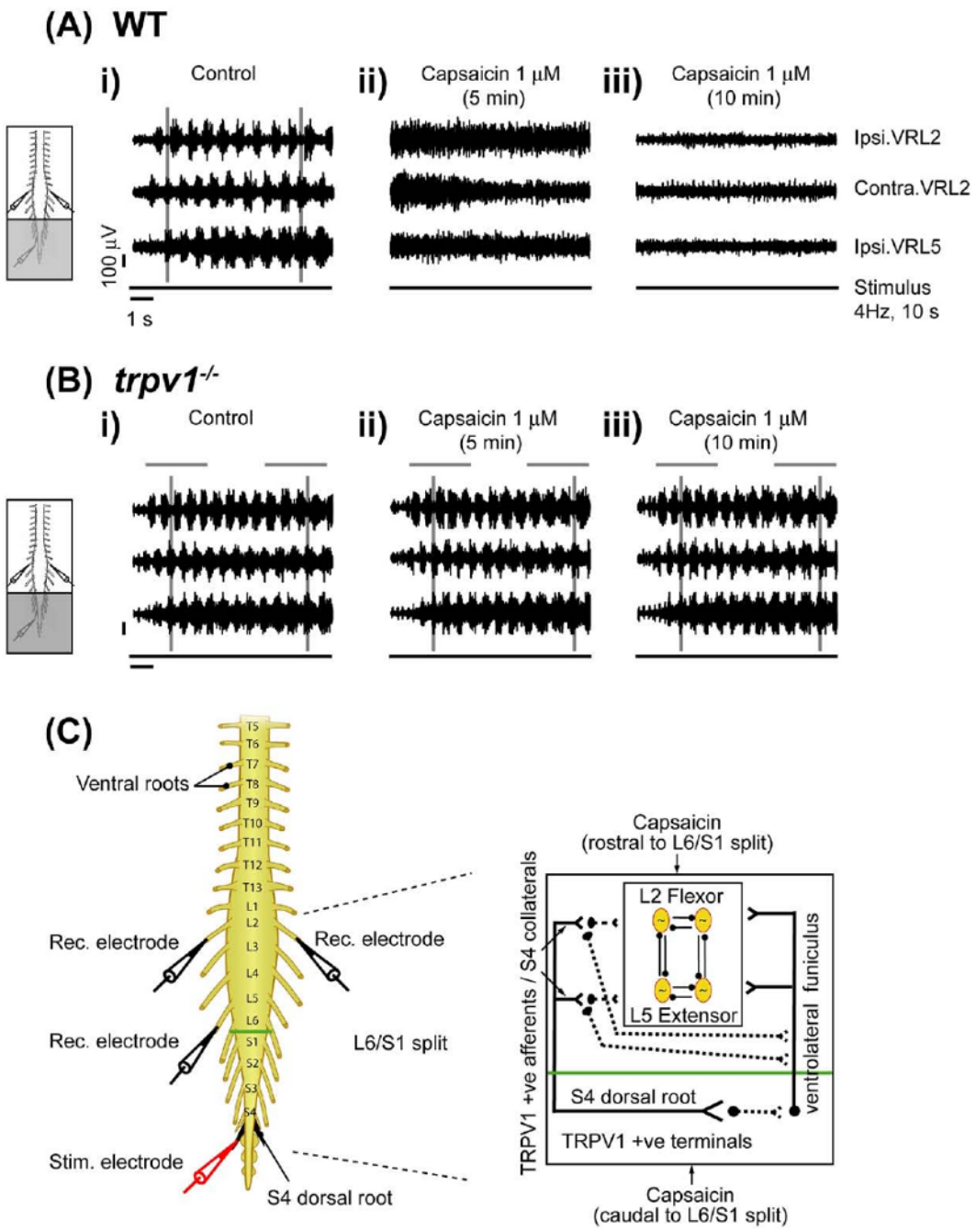


**Fig. 2.**

Capsaicin modulation of SCA-evoked locomotor rhythm via TRPV1. Stimulation of the S4 dorsal root can evoke alternating rhythmic discharge from L2 and L5 ventral roots in wild type and *trpv1*$^{-/-}$ isolated spinal cord preparations, transected at T5. A split-bath was built with Vaseline walls between S1 and L6. Capsaicin was bath applied to the caudal compartment (S1 to cauda equina) of the split bath (grey shaded area). All neurograms were recorded from right L2 (Ipsi. VRL2), left L2 (Contra. VRL2) and right ventral L5 roots (Ipsi. VRL5). Ipsilateral (Ipsi.) and contralateral (Contra.) are abbreviations used for ventral root recordings relative to the side of dorsal root stimulation. The line below each set of neurograms indicates the duration of the train of stimuli applied to the S4 dorsal root (4 Hz, 10 s, 2 T). The voltage and time scales

shown in data set Ai are common to all traces in the figure. Vertical grey lines highlight alternating rhythmic discharge of the neurograms. Horizontal grey lines highlight selected number of bursts within the neurogram. (A) Effect of caudal application of capsaicin in wild type preparations. (i) Rhythmic neurogram discharges in untreated control conditions. (ii) Uncoordinated neurogram discharge within 5 min of capsaicin (1 $\mu$M) application to the caudal compartment. (iii) Complete blockade of ventral root neurogram discharges following 10 min of continued capsaicin (1 $\mu$M) application in the same preparation ($n$=5). (B) Effect of caudal application of capsaicin in *trpv1*$^{-/-}$ preparations. (i) Rhythmic neurogram discharges in untreated control conditions. (ii) No change in neurogram discharges within 5 min of capsaicin (1 $\mu$M) application to the caudal compartment. (iii) Lack of blockade of neurogram discharges following 10 min of capsaicin (1 $\mu$M) application in the same preparation ($n$=3). (C) Schematic diagram representing the neonatal mouse spinal cord preparations used. There is the stimulation electrode (red) at dorsal S4 root (black) and recording electrodes (black) at right and left L2 and right L5 right ventral roots. A split-bath was built with a Vaseline wall (green) between the L6 and S1 segments. The inset schematic presents the hypothesis that capsaicin application to the caudal compartment of L6/S1 split targets either sacral capsaicin sensitive TRPV1 positive afferent terminals projecting onto lumbar motor networks by way of intercalated interneurons in the VLF or TRPV1 positive S4 afferent collaterals from sacral segments onto lumbar segments via dorsolateral tracts. Capsaicin application to the rostral compartment of the L6/S1 split bath targets TRPV1 positive S4 afferent collaterals originating from sacral segments onto lumbar segments. These TRPV1 positive afferents can rostrocaudally modulate lumbar locomotor CPG networks which may include polysynaptic projections onto the VLF. For interpretation of the references to color in this figure legend, the reader is referred to the Web version of this article.

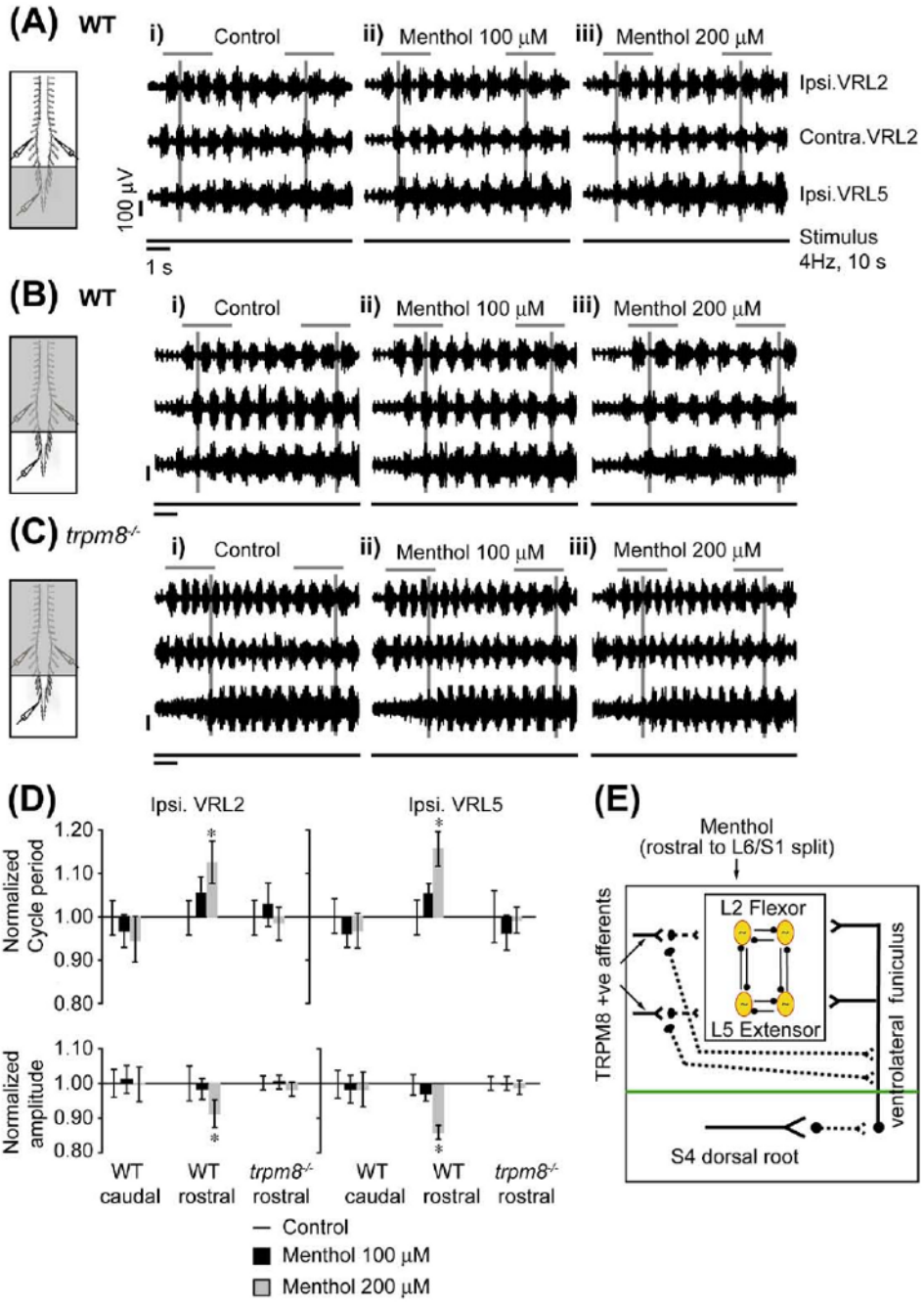


**Fig. 3.**

Menthol modulation of SCA-evoked locomotor rhythm via TRPM8. Stimulation of the S4 dorsal root can evoke alternating rhythmic discharge from L2 and L5 ventral roots in wild type and *trpm8*$^{-/-}$ spinal cord preparations, transected at T5. A split-bath was built with Vaseline walls between S1 and L6. Menthol (grey shaded area) was bath-applied to the caudal or rostral compartments of the split-bath. All neurograms were recorded from the right L2 (Ipsi. VRL2), left L2 (Contra. VRL2) and right L5 (Ipsi. VRL5) ventral roots. Ipsilateral (Ipsi.) and contralateral (Contra.) are abbreviations used for ventral root recordings relative to the side of dorsal root stimulation. The line below each set of neurograms indicates the duration of the train of stimuli applied to the S4 dorsal root (4 Hz, 10 s, 2 T). The voltage and time scales

shown in data set Ai are common to all traces in the figure. The vertical grey lines indicate alternating rhythmic discharge of the ventral roots. Horizontal grey lines are drawn to highlight a selected number of bursts within the neurogram. (A) Effect of caudal application of menthol in wild type preparations. (i) Rhythmic ventral root discharges in untreated control conditions. (ii, iii) No change in neurogram discharge following a 15 min menthol (100 and 200 $\mu$M) application to the caudal compartment of the split bath ($n$=3). (B) Effect of rostral application of menthol in wild type preparations. (i) Rhythmic neurogram discharge in untreated control conditions. (ii) The rhythm is unaffected following 15 min of bath application of menthol (100 $\mu$M). (iii) Significant increase in the cycle period and decrease in the amplitude of neurogram rhythmic discharges following 15 min of bath application of menthol (200 $\mu$M) in the same preparation ($n$=3). (C) Effect of rostral application of menthol in *trpm8*$^{-/-}$ preparations. (i) Alternating left and right rhythmic neurogram discharges in untreated control conditions. (ii) The rhythm is unaffected following a 15 min bath application of menthol (100 $\mu$M). (iii) Increase in cycle period and decrease in amplitude of neurogram bursting activity is attenuated following 15 min of bath application of menthol (200 $\mu$M) compared to wild type preparations ($n$=4). (D) The top panel histogram bar graph shows a significant increase in the cycle period of the SCA-evoked rhythm when 200 $\mu$M of menthol is applied in the rostral compartment in spinal cord preparations from wild type but not *trpm8*$^{-/-}$ mice. No change in cycle period was observed when menthol was applied in the caudal compartment of spinal cord preparations from WT mice. All data were normalized to 1. The bottom panel histogram bar graph shows a significant decrease in the burst amplitude of the SCA-evoked rhythm when 200 $\mu$M of menthol is applied in the rostral compartment in spinal cord preparations from WT but not *trpm8*$^{-/-}$ mice. No change in burst amplitude was observed when menthol was applied in the caudal compartment preparations from wild type mice. All data were normalized to 1. * Significant difference (two-way ANOVA with repeated measures, $P$<0.05). (E) The schematic presents the hypothesis that menthol (200 $\mu$M) application to the rostral compartment targets TRPM8 positive afferent terminals of lumbar segments. Activation of these TRPM8 positive afferents can modulate lumbar locomotor CPG networks polysynaptically which may include polysynaptic projections onto the VLF. On the other hand, menthol application to the caudal compartment does not affect lumbar motor networks via the SCA pathways. For interpretation of the references to color in this figure legend, the reader is referred to the Web version of this article.

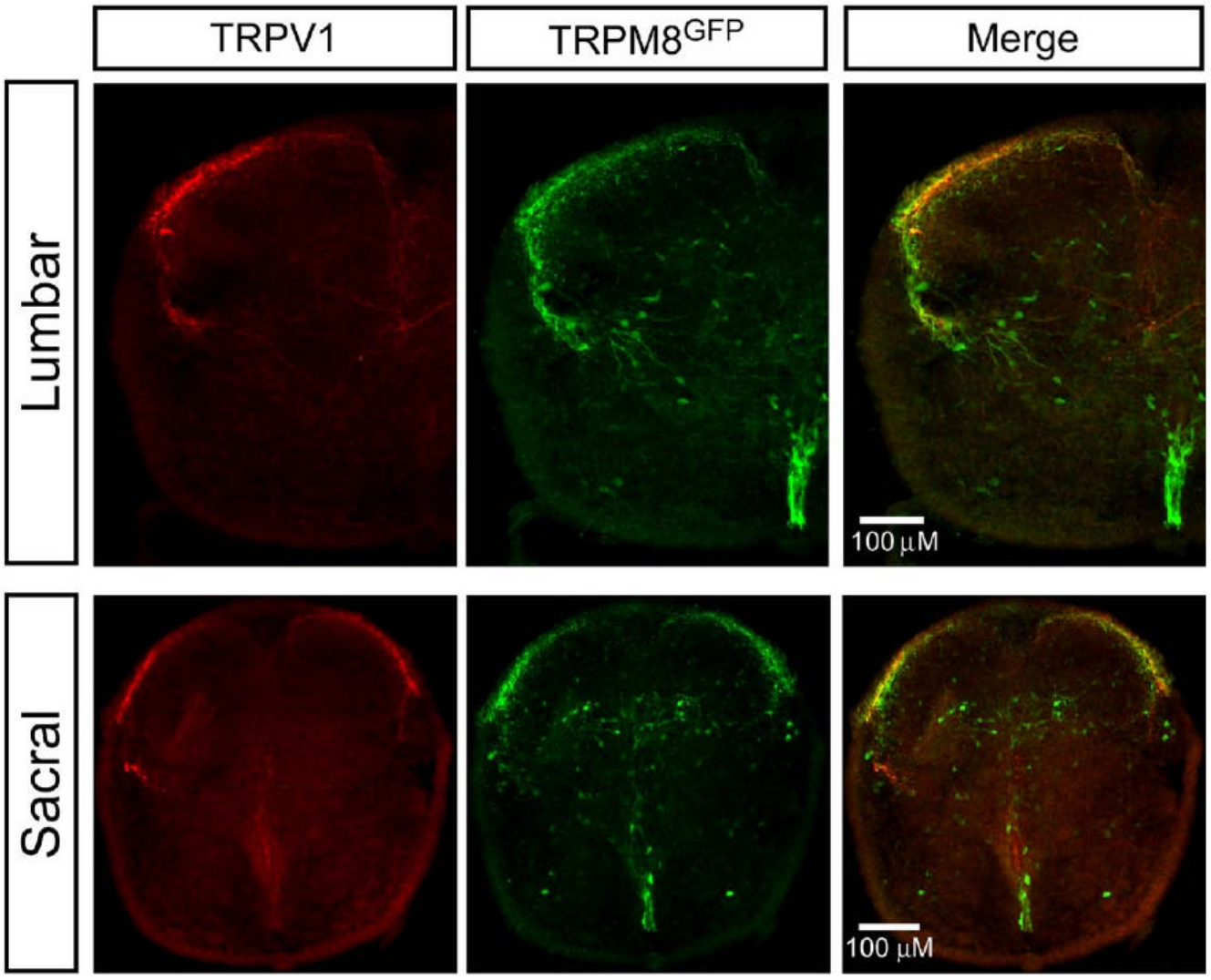


**Fig. 4.**

TRPV1 and TRPM8 expression in lumbar and sacral segments. Representative immunohistochemistry showing TRPV1 and TRPM8 expression in lumbar and sacral segments of spinal cord sections (30 $\mu$M) obtained from P0–P3 TRPM8-GFP transgenic mice. TRPV1 expression (red fluorescence, left panel) was restricted to the dorsal horn in both lumbar and sacral segments. TRPM8-GFP expression (green fluorescence, middle panel) was present in dorsal horn and ventral horn midline below the central canal in lumbar and sacral segments. Merged images (right panel) showed some co-localization of TRPV1 and TRPM8-GFP (yellow) in the dorsal horn of both lumbar and sacral segments. For interpretation of the references to color in this figure legend, the reader is referred to the Web version of this article.

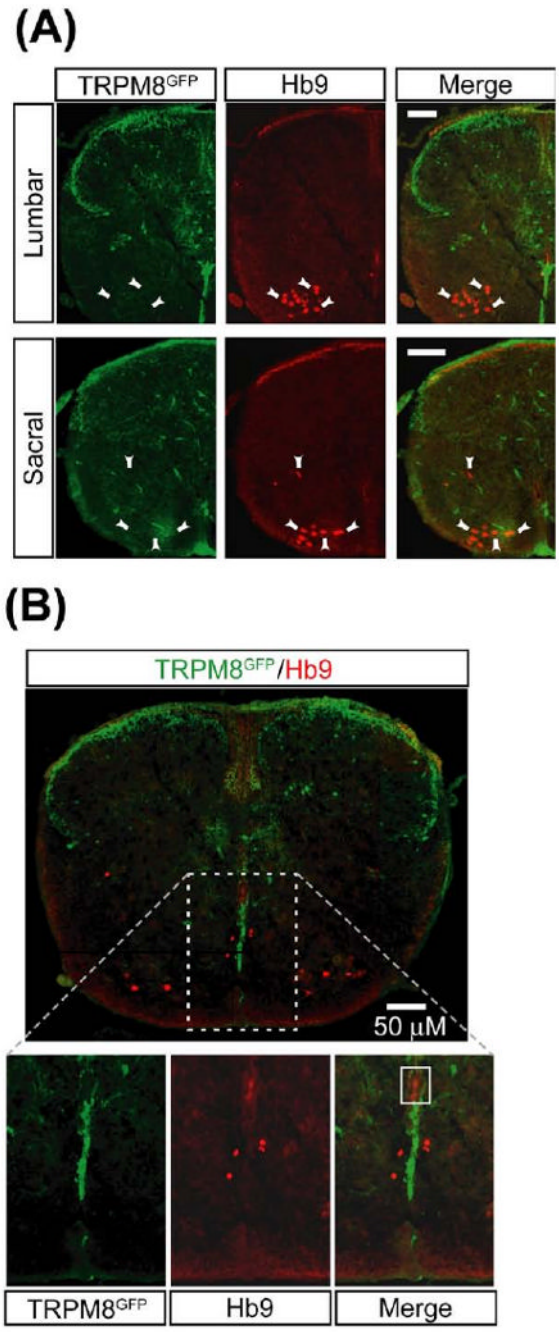


**Fig. 5.**

TRPM8 does not co-localize with Hb9 positive motoneurons or putative CPG interneurons. Representative immunohistochemistry showing TRPM8 expression and Hb9 positive motoneurons and interneurons in the ventral horn of lumbar and sacral segments of spinal cord sections (30 $\mu$M) obtained from P0–P3 TRPM8-GFP transgenic mice. (A) Images of TRPM8-GFP (green color, left panel) and Hb9 positive motoneurons (red color, middle panel, arrowheads) in both lumbar and sacral segments. No co-localization between TRPM8-GFP and motoneurons was seen as shown in merged images (right panel). Scale bars=50 $\mu$M. (B) Top panel represents lumbar segments showing merged image of TRPM8 expression (green) and Hb9 positive interneurons (red). There was no co-localization between TRPM8-GFP and

interneurons expressing Hb9. There was close proximity between TRPM8-GFP expression in ventral midline below the central canal and interneurons expressing Hb9. Bottom panels represent images at higher magnification. No co-localization was seen even at higher magnifications. For interpretation of the references to color in this figure legend, the reader is referred to the Web version of this article.

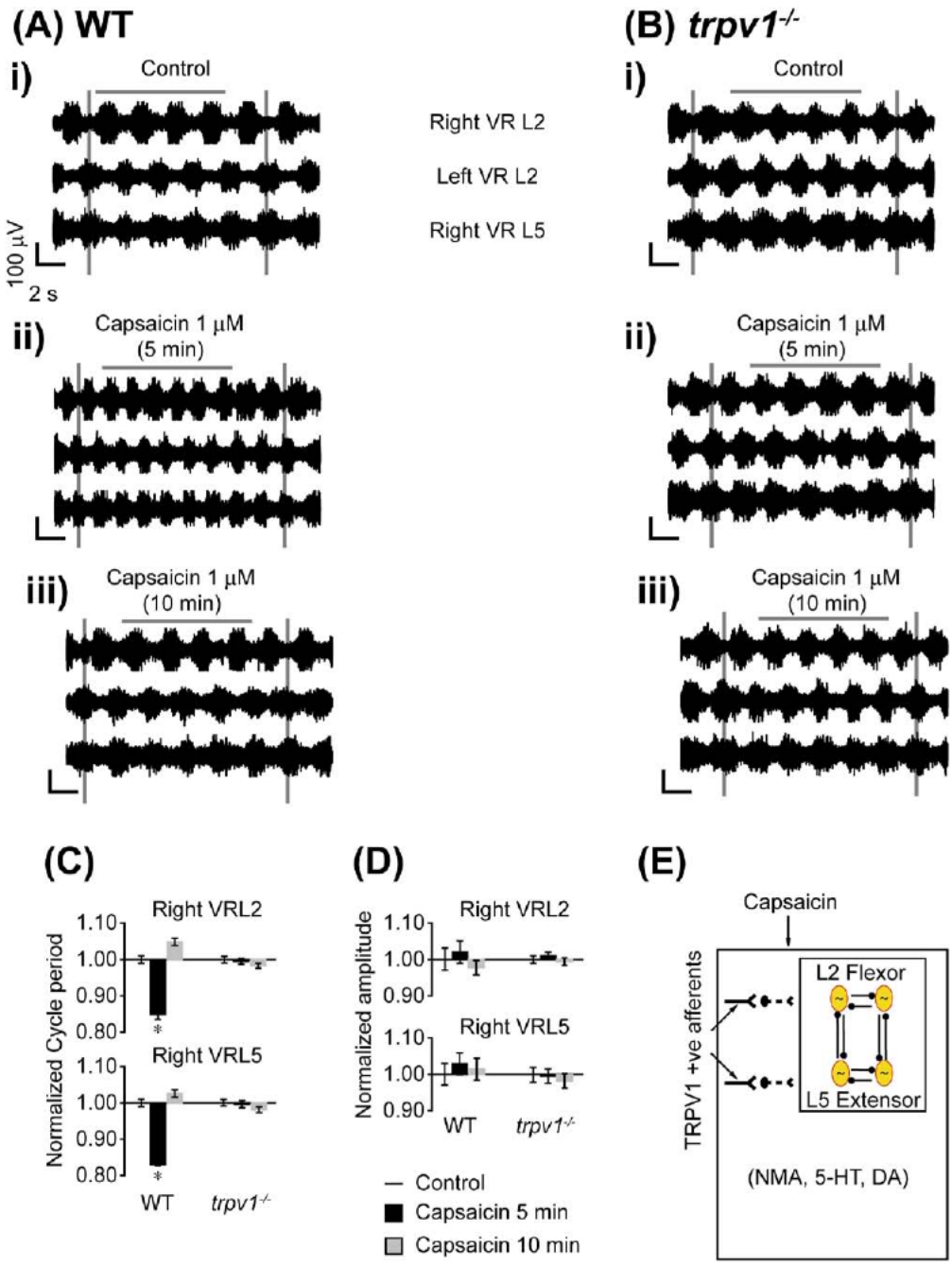


**Fig. 6.**

Capsaicin modulation of drug-evoked locomotor rhythm via TRPV1. Bath application of capsaicin affects drug-evoked rhythmic activity in wild type but not *trpv1*$^{-/-}$ mice. NMA (5 $\mu$M), 5-HT (10 $\mu$M), and DA (50 $\mu$M) were bath-applied to whole spinal cord preparations transected at T5 to elicit rhythmic activity. The neurograms shown were band-pass filtered (0.1–1 kHz) traces recorded from the right and left L2s (Right VRL2; Left VRL2) and right L5 (Right VRL5) ventral roots. The voltage and time scales shown in data set Ai are common to all traces in the figure. Vertical grey lines are drawn to highlight alternating rhythmic discharge of the neurograms. Horizontal grey lines are drawn to highlight a selected number of bursts within the neurogram. (A) Effects of capsaicin on wild type preparations ($n$=5). (i)

Rhythmic neurogram discharges in control conditions. (ii) Bath application of capsaicin (1 $\mu$M) results in a significant increase in frequency (reduced cycle period) of neurogram discharges within 5 min. (iii) A return to control frequency of ventral root discharges following 10 min of continued capsaicin (1 $\mu$M) application in the same preparation. (B) Effects of capsaicin on *trpv1*$^{-/-}$ preparations ($n$=3). (i) Rhythmic ventral root discharges in control conditions. (ii, iii) No change in neurogram discharge frequency or amplitude within 5 or 10 min of capsaicin (1 $\mu$M) application. (C) Histogram bar graph showing capsaicin causing a significant decrease in cycle period of drug-evoked rhythm in spinal cord preparations from wild type but not *trpv1*$^{-/-}$ mice. * Significant difference (ANOVA by repeated measures, $P$<0.05). (D) Histogram bar graph showing capsaicin has no significant effect in burst amplitude in spinal cord preparations from WT and *trpv1*$^{-/-}$ mice. All data were normalized to 1. (E) Schematic diagram presents the hypothesis that the capsaicin sensitive and TRPV1 positive afferents can modulate lumbar locomotor CPG networks activated by the combination of rhythmogenic drugs NMA, 5-HT and DA. For interpretation of the references to color in this figure legend, the reader is referred to the Web version of this article.

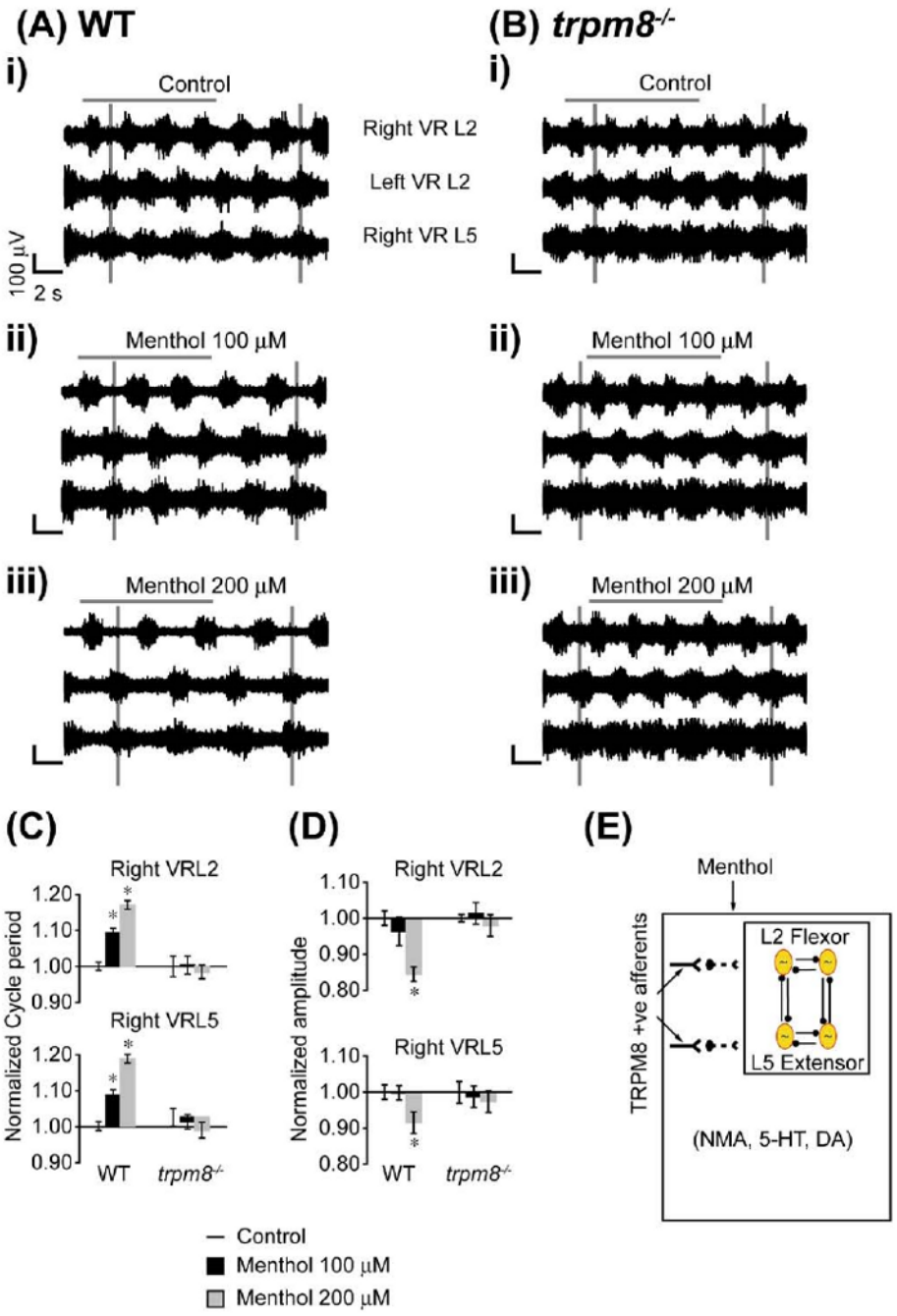


**Fig. 7.**

Menthol modulation of drug-evoked locomotor rhythm via TRPM8. Bath application of menthol affects drug-evoked rhythmic activity in wild type but not *trpm8*$^{-/-}$ mice. NMA (5 $\mu$M), 5-HT (10 $\mu$M), and DA (50 $\mu$M) were bath-applied to isolated spinal cord preparations transected at T5 to elicit rhythmic activity. The neurograms shown were band-pass filtered (0.1–1 kHz) traces recorded from right and left L2s (Right VRL2; Left VRL2) and right L5 (Right VRL5) ventral roots. The voltage and time scales shown in data set Ai are common to all traces in the figure. Vertical grey lines are drawn to highlight alternating rhythmic discharge of the neurograms. Horizontal grey lines are drawn to highlight selected number of bursts within the neurogram. (A) Effect of menthol on wild type preparations ($n$=5). (i) Rhythmic

neurogram discharges under control conditions. (ii) Significant increase in the cycle period of rhythmic bursts following 15 min of bath application of menthol (100 $\mu$M). There was no change in burst amplitude. (iii) Further significant increase in the cycle period and significant decrease in burst amplitude recorded 15 min following bath application of menthol (200 $\mu$M) in the same preparation. (B) Effect of menthol on *trpm8*$^{-/-}$ preparations ($n$=4). (i) Rhythmic ventral root discharges under control conditions. (ii) No change in neurogram discharge frequency or amplitude following a 15 min bath application of menthol (100 $\mu$M). (iii) No change in neurogram discharge frequency or amplitude following a 15 min bath application of menthol (200 $\mu$M) in the same preparation. (C) Histogram bar graph showing menthol causing a significant dose dependent increase in the cycle period of drug-evoked rhythm in spinal cord preparations from wild type but not *trpm8*$^{-/-}$ mice. (D) Histogram bar graph showing menthol (200 $\mu$M) causing a significant decrease in burst amplitude in spinal cord preparations from wild type but not *trpm8*$^{-/-}$ mice. * Significant difference ($P$<0.05). All data were normalized to 1. (E) Schematic diagram presents the hypothesis that the menthol sensitive and TRPM8 positive afferents can modulate lumbar locomotor CPG networks activated by the combination of rhythmogenic drugs NMA, 5-HT and DA. For interpretation of the references to color in this figure legend, the reader is referred to the Web version of this article.

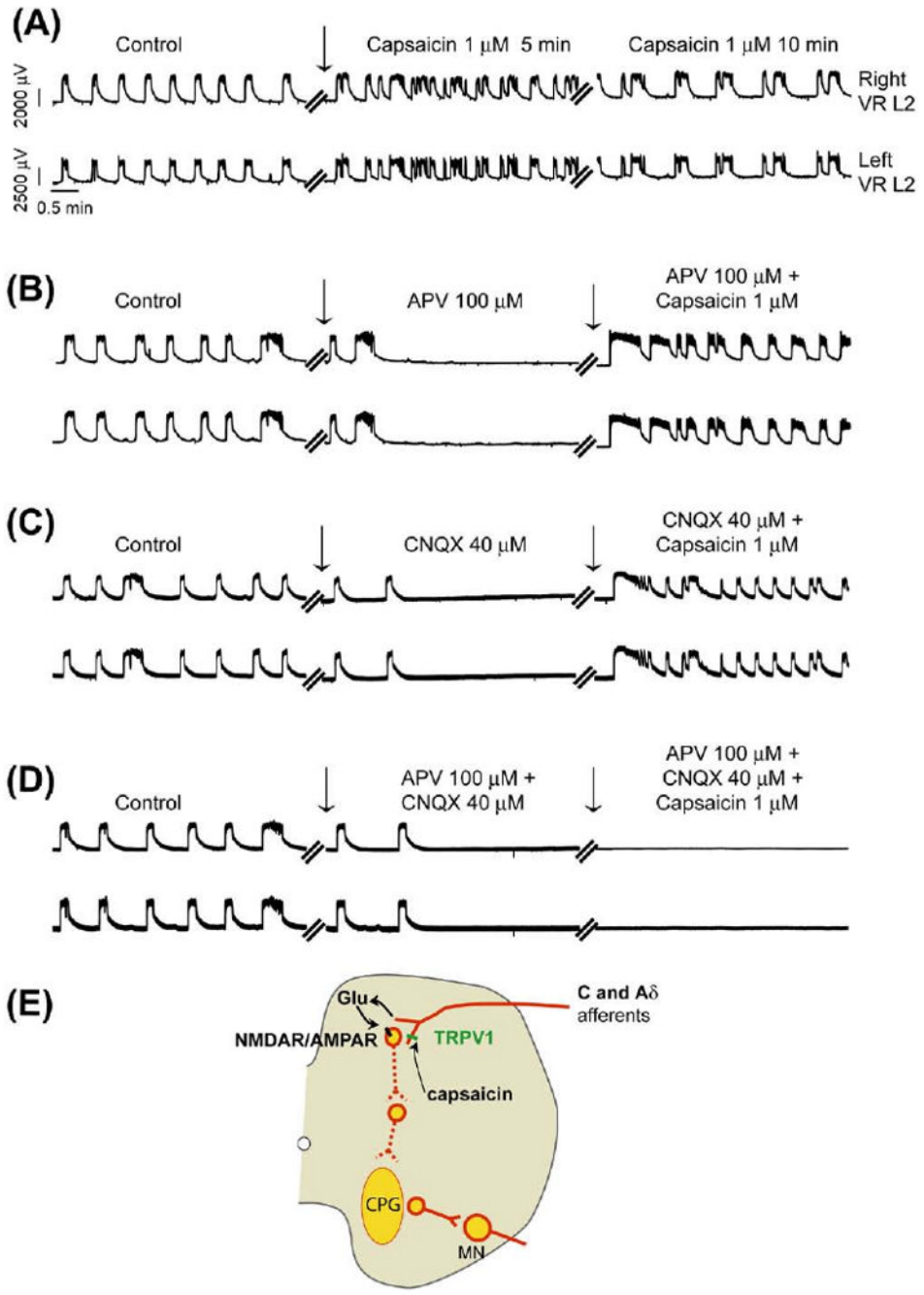


**Fig. 8.**

Capsaicin modulation of synchronous locomotor rhythm via excitatory glutamatergic mechanism. Synchronous disinhibited rhythmic activity was evoked by bath application of strychnine (2 $\mu$M), picrotoxin (50 $\mu$M), and CGP (50 $\mu$M) to isolated wild type spinal cord preparations transected at T5 ($n$=4). All neurograms shown here were recorded (DC −1 kHz) from the left and right L2 (right and left VR L2) ventral roots. The voltage and time scales shown in data set Ai are common to all traces in the figure. Vertical arrows in all neurograms indicate the point of drug applications. (A) A significant increase in frequency of neurogram oscillations is shown within 5 min following bath application of capsaicin (1 $\mu$M), which declined after 10 min of continued capsaicin (1 $\mu$M) application to the same preparation. (B)

Application of APV (100 $\mu$M) completely inhibited the synchronous rhythm. Recovery of the disinhibited synchronous rhythm was observed upon capsaicin (1 $\mu$M) application to the whole cord. (C) Application of CNQX (40 $\mu$M) completely inhibited the synchronous rhythm. Recovery of the disinhibited synchronous rhythm was observed upon capsaicin (1 $\mu$M) application. (D) Application of APV (100 $\mu$M) and CNQX (40 $\mu$M) completely inhibited the synchronous rhythm. There was no recovery of the disinhibited synchronous rhythm following bath application of capsaicin (1 $\mu$M) to the whole cord. (E) The schematic diagram represents the proposed mechanism of capsaicin-induced modulation of locomotor CPG via excitatory glutamatergic synaptic transmission. Capsaicin is proposed to activate the TRPV1 receptors on the afferent terminals in the dorsal horn to release glutamate (Glu), which in turn activates the postsynaptic NMDAR/AMPAR complex. This excitatory glutamatergic mechanism then polysynaptically targets the locomotor CPG. For interpretation of the references to color in this figure legend, the reader is referred to the Web version of this article.

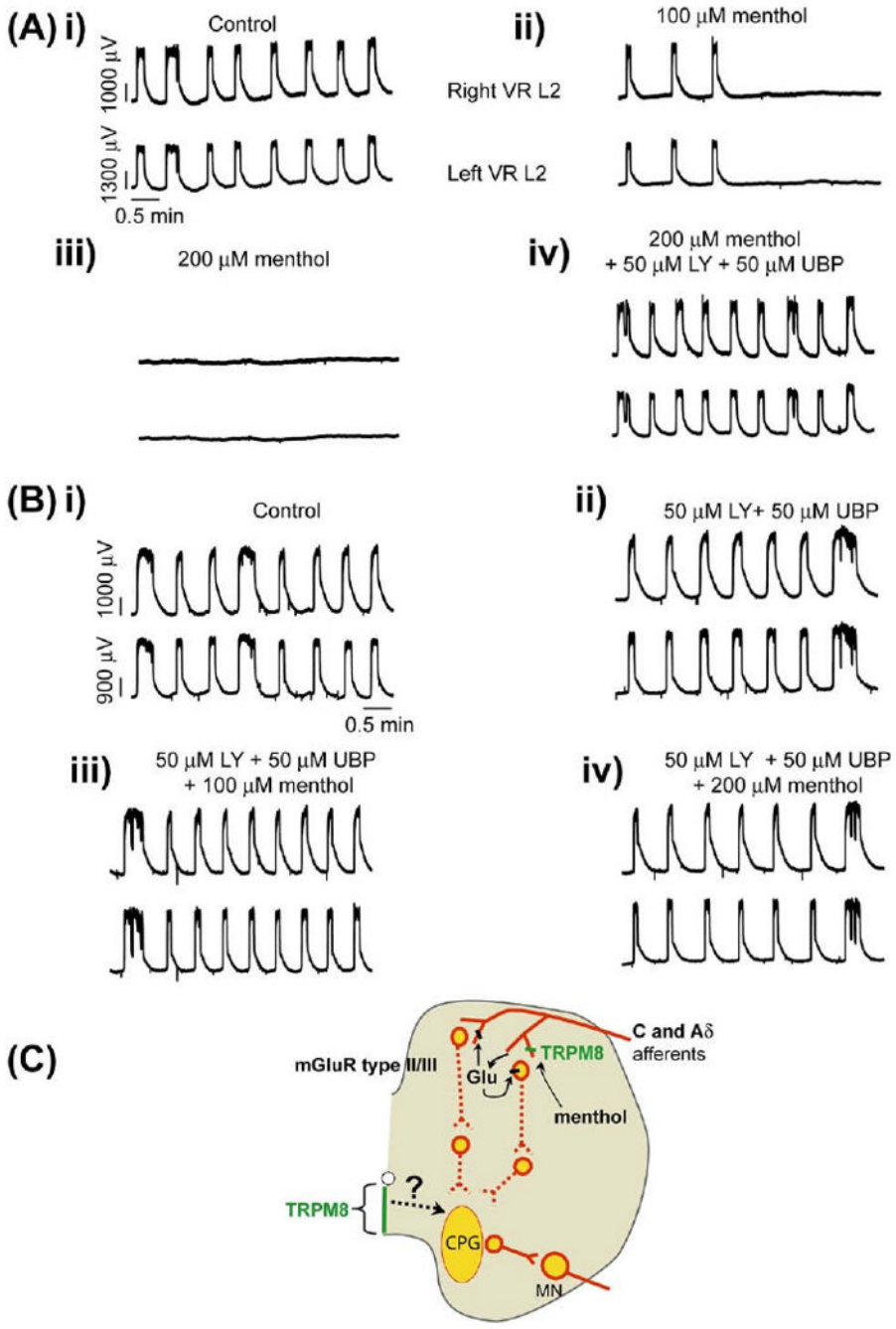


**Fig. 9.**

Menthol modulation of synchronous locomotor rhythm via inhibitory glutamatergic mechanisms. Synchronous disinhibited ventral root rhythmic activity is evoked by bath application of strychnine (2 $\mu$M), picrotoxin (50 $\mu$M), and CGP (50 $\mu$M) to isolated spinal cord preparations transected at T5. The neurograms shown are DC traces recorded from the right and left (right and left VR L 2) ventral roots. The voltage and time scales shown in the data set Ai are common to all traces in the figure. (A) Synchronous left and right rhythmic neurogram oscillations in control conditions. (ii, iii) Bath application of menthol (100 $\mu$M and 200 $\mu$M) to the same preparation inhibited rhythmic oscillations. (iv) Effect of menthol (200 $\mu$M) was reversed by bath application of the mGluR type I antagonist LY341495 (50 $\mu$M) and the mGluR

type II antagonist UBP1112 (50 $\mu$M) to the same preparation ($n$=6). (Bi) Synchronous left and right rhythmic ventral root oscillations under control conditions. (ii) Application of LY341495 (50 $\mu$M) and UBP1112 (50 $\mu$M) did not alter the rhythm. (iii, iv) Attenuation of oscillatory neurogram activity by menthol (100 and 200 $\mu$M) was blocked in the presence of LY341495 (50 $\mu$M) and UBP1112 (50 $\mu$M) ($n$=6). (C) The schematic diagram represents the proposed mechanism of menthol induced modulation of locomotor CPG via inhibitory glutamatergic synaptic transmission. Menthol is proposed to activate the TRPM8 receptors on the afferent terminals in the dorsal horn to release glutamate (Glu), which then acts through inhibitory Group II/III mGluR receptors located either presynaptically on menthol-activated TRPM8+ afferents or possibly postsynaptically on dorsal horn neurons. This inhibitory glutamatergic mechanism then polysynaptically targets the locomotor CPG. Projections between ventromedial TRPM8 and spinal motor centers are unknown. For interpretation of the references to color in this figure legend, the reader is referred to the Web version of this article.

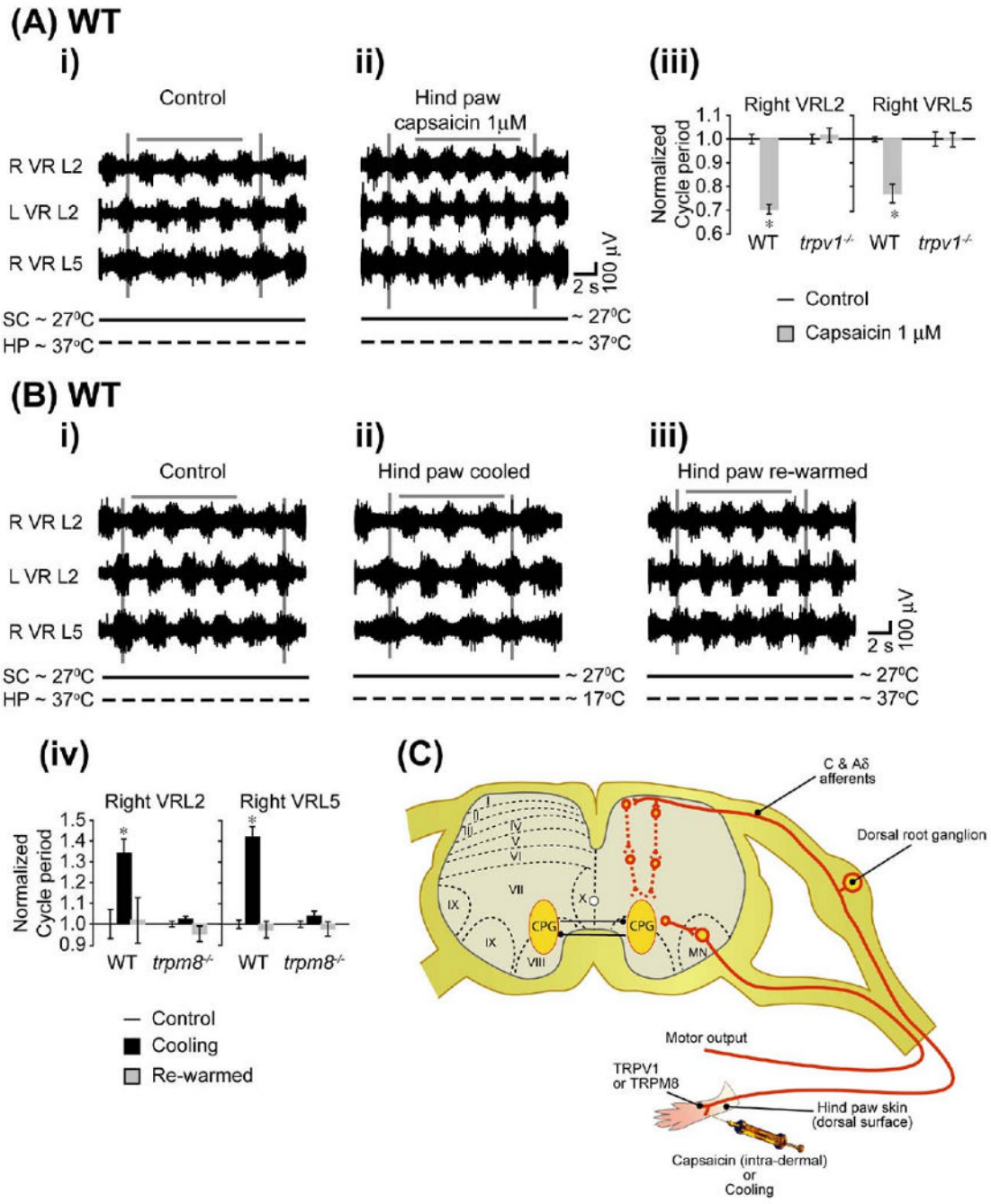


**Fig. 10.**

Peripheral stimulation of TRPV1 and TRPM8 modulates drug-evoked locomotor rhythm. Hind limb–attached spinal cord preparations transected at T5 with intact lumbar dorsal root connections to hind limb were obtained from wild type, *trpv1*$^{-/-}$ and *trpm8*$^{-/-}$ mice. The hind paw was separated from the spinal cord by building a Vaseline wall as indicated in the Experimental Procedures. Ventral root rhythmic activity was evoked by bath application of NMA(5 $\mu$M), 5-HT (10 $\mu$M), and DA (50 $\mu$M) to the spinal cord section of the split bath. The hind paw was stimulated by intra-dermal capsaicin for TRPV1 activation or cold bath solution for TRPM8 activation. The neurograms shown were band-pass filtered (0.1–1 kHz) traces recorded from the right L2 (R VRL2), left L2 (L VRL2) and right L5 (R VRL5) ventral roots.

The voltage and time scales shown in the data set are common to all traces in the figure. Vertical grey lines are drawn to highlight alternating rhythmic discharge of the neurograms. Horizontal grey lines are drawn to highlight a selected number of bursts within the neurogram. The solid horizontal black line below each neurogram represents temperature at the spinal cord section (SC ~27 °C) and the dotted horizontal black line represents various temperatures in the hind paw (HP) section. (A) Effect of intra-dermal capsaicin stimulus in wild type preparations ($n$=4). (i) Rhythmic neurogram discharges under control conditions (SC ~27 °C, HP ~32 °C). (ii) Significant decrease in the cycle period of neurogram discharges within 5 min of capsaicin (1 $\mu$M) application to the hind paw. (iii) Histogram bar graph showing a significant decrease in the cycle period of the drug-evoked rhythm by capsaicin applied to the hind paw in WT but not *trpv1*$^{-/-}$ mice. * Significant difference (paired $t$-test, $P$<0.05). All data were normalized to 1. (B) Effect of cold bath solution stimulus in wild type preparations ($n$=4). (i) Rhythmic neurogram discharges in control conditions (SC ~27 °C, HP ~32 °C). (ii) There is a significant increase in cycle period of neurogram discharges during cold bath (~17 °C) application to the hind paw. (iii) The cycle period returned to control values when the hind paw was warmed up to control conditions (~32 °C). (iv) Histogram bar graph showing a significant increase in the cycle period of the drug-evoked rhythm during cooling of the hind paw in wild type but not *trpm8*$^{-/-}$ mice. * Significant difference (ANOVA by repeated measures, $P$<0.05). All data were normalized to 1. (C) Schematic diagram illustrating stimulation of peripheral TRPV1 by capsaicin or TRPM8 by cooling, classes of afferents, and possible connectivity within the spinal cord. For interpretation of the references to color in this figure legend, the reader is referred to the Web version of this article.

**Table 1**

Capsaicin has no direct action on motoneurons

| **Motoneuron properties** | **Control** | **Capsaicin 1 $\mu$M** |
|---|---|---|
| Action potential amplitude (mV) | 79.36±6.07 | 78.11±6.89 |
| Voltage threshold (mV) | −35.75±0.57 | −39.18±2.06 |
| Rheobase current (pA) | 226.50±13.36 | 201.40±12.46 |
| After-hyperpolarization half-decay time (ms) | 46.93±5.96 | 49.97±3.38 |
| Input resistance (Mohm) | 88.37±8.79 | 96.04±9.04 |
| f-I Gain (Hz/nA) | 56.29±4.38 | 57.26±7.56 |
| Initial inter-spike interval slope (ms/nA) | −304.60±42.46 | −306.70±44.10 |

Whole-cell motoneuron recordings in lumbar L4–L5 segments were obtained from spinal cord slices of wild type mice. Capsaicin (1 $\mu$M) had no significant effect on any of the motoneuron properties listed in the table ($n$=8 motoneurons).

## Table 2

Menthol has no direct action on motoneurons

| Motoneuron properties | Control | |
|---|---|---|
| | | Menthol 100 $\mu$M |
| Action potential amplitude (mV) | 78.15±1.21 | 75.97±1.52 |
| Voltage threshold (mV) | −42.34±3.72 | −40.63±1.05 |
| Rheobase current (pA) | 204.90±21.05 | 180.30±20.70 |
| After-hyperpolarization half-decay time (ms) | 44.93±5.27 | 49.32±5.11 |
| Input resistance (Mohm) | 73.57±8.79 | 73.41±8.60 |
| f-I Gain (Hz/nA) | 63.75±7.13 | 62.81±5.94 |
| Initial inter-spike interval slope (ms/nA) | −271.10±81.85 | −306.80±30.00 |
| | | Menthol 200 $\mu$M |
| Action potential amplitude (mV) | 77.95±2.28 | 75.97±2.43 |
| Voltage threshold (mV) | −40.56±1.31 | −44.35±1.33 |
| Rheobase current (pA) | 213.30±18.59 | 184.10±18.35 |
| After-hyperpolarization half-decay time (ms) | 41.95±4.01 | 46.26±4.35 |
| Input resistance (Mohm) | 82.52±13.17 | 85.71±15.29 |
| f-I Gain (Hz/nA) | 64.26±6.70 | 59.21±5.94 |
| Initial inter-spike interval slope (ms/nA) | −313±54.24 | −280.90±55.93 |

Whole-cell motoneuron recordings in lumbar L4–L5 segments were obtained from spinal cord slices of wild type mice. Menthol at both 100 $\mu$M (top table, $n$=9 motoneurons) and 200 $\mu$M (bottom table, $n$=10 motoneurons) had no significant effect on any of the motoneuron properties listed in the table.